MOLECULAR AND CELLULAR BIOLOGY, Sept. 2011, p. 3569–3583 Vol. 31, No. 17
0270-7306/11/$12.00 doi:10.1128/MCB.05590-11
Copyright © 2011, American Society for Microbiology. All Rights Reserved.

H3K4 Trimethylation by Set1 Promotes Efficient Termination by the Nrd1-Nab3-Sen1 Pathway▽†

Nihal Terzi,[1] L. Stirling Churchman,[2] Lidia Vasiljeva,[1]‡
Jonathan Weissman,[2] and Stephen Buratowski[1]*

Department of Biological Chemistry and Molecular Pharmacology, Harvard Medical School, Boston, Massachusetts 02115,[1] *and Department of Cellular and Molecular Pharmacology, Howard Hughes Medical Institute, University of California, San Francisco, and California Institute for Quantitative Biosciences, San Francisco, California 94158*[2]

Received 4 May 2011/Returned for modification 1 June 2011/Accepted 15 June 2011

In *Saccharomyces cerevisiae*, the Nrd1-Nab3-Sen1 pathway mediates the termination of snoRNAs and cryptic unstable transcripts (CUTs). Both Nrd1 and the Set1 histone H3K4 methyltransferase complex interact with RNA polymerase II (Pol II) during early elongation, leading us to test whether these two processes are functionally linked. The deletion of *SET1* exacerbates the growth rate and termination defects of *nrd1* mutants. Set1 is important for the appropriate recruitment of Nrd1. Additionally, Set1 modulates histone acetylation levels in the promoter-proximal region via the Rpd3L deacetylase and NuA3 acetyltransferase complexes, both of which contain PHD finger proteins that bind methylated H3K4. Increased levels of histone acetylation reduce the efficiency of Nrd1-dependent termination. We speculate that Set1 promotes proper early termination by the Nrd1-Nab3-Sen1 complex by affecting the kinetics of Pol II transcription in early elongation.

From initiation through termination, transcript synthesis by RNA polymerase II (Pol II) is coupled to RNA processing and quality control. One mechanism for the temporal coordination of these processes is via the modification of Pol II itself. The C-terminal domain (CTD) of the Pol II subunit Rpb1 consists of multiple tandem repeats of the sequence YSPTSPS. Close to the promoter during early elongation, the serines at positions 5 (S5) and 7 (S7) of the repeat are phosphorylated by the kinase subunit of the basal factor TFIIH (reviewed in reference 8). Later in elongation, serine 2 (S2) is phosphorylated by the yeast Bur1 and Ctk1 kinases or their metazoan homologs Cdk9 (13, 28, 31, 44) and Cdk12 (4). The dynamic CTD phosphorylation patterns direct the recruitment of the appropriate RNA-processing and chromatin modification factors at different stages of transcription.

snoRNAs, some short mRNAs, and the recently discovered class of cryptic unstable transcripts (CUTs) are terminated in yeast via the Nrd1-Nab3-Sen1 pathway (3, 25, 51, 52, 56). Unlike mRNAs that undergo 3′ polyadenylation, transcripts terminated by the Nrd1-Sen1 pathway are directed to the nuclear exosome complex for 3′-end trimming or degradation (59). It is thought that the Sen1 helicase mediates termination after being brought to the transcript by the sequence-specific RNA binding proteins Nrd1 and Nab3 (10, 50). The Nrd1 and Nab3 recognition sequences are short, and their presence and frequency vary between Nrd1 target genes. However, these sites also appear in genes that are not terminated by the Nrd1-Sen1 pathway. Further biasing the complex to short genes is the interaction of the Nrd1 CTD interaction domain (CID) with the S5-phosphorylated CTD in promoter-proximal regions (17, 60). Therefore, it is the combination of the CTD interaction and RNA recognition that ensures the proper loading of the complex and subsequent transcription termination. Defects in the recruitment of the Nrd1-Sen1 complex result in read-through transcription and 3′-processing defects (60).

Transcription initiation and elongation can be influenced by histone modifications and chromatin dynamics. Examples include the deacetylation of histones by Sir2 to create repressive heterochromatin (37, 38) and the methylation of histone H3 at lysine 36 (H3K36) by Set2, which recruits the Rpd3S histone deacetylase (HDAC) complex to suppress cryptic initiation and slow elongation within mRNA genes (11, 24, 30). There are suggestions that chromatin may also play a role in the transcription termination of polyadenylated mRNA genes (2, 39). Since Nrd1-dependent termination occurs in the promoter-proximal region, we asked whether histone modifications in this region might affect snoRNA or CUT termination.

The trimethylation of histone 3 at lysine 4 (H3K4) by the histone methyltransferase Set1 (6) is highly enriched in promoter-proximal regions of actively transcribed genes, while H3K4me2 peaks slightly further downstream (26, 42). Set1 is recruited to early transcription elongation complexes coincident with the S5-phosphorylated CTD (41). Given that the peak of H3K4 trimethylation (H3K4me3) coincides with the region of Nrd1 recruitment, we tested whether H3K4 methylation affects Nrd1-dependent termination and found that the deletion of *SET1* exacerbates the termination defects of *nrd1* mutants. Set1-mediated H3K4 trimethylation contributes to Nrd1-dependent termination by promoting Nrd1 recruitment. The recognition of H3K4 trimethylation by several PHD finger proteins helps maintain balanced histone acetylation levels, which influence the kinetics of Pol II transcription and thereby

* Corresponding author. Mailing address: Department of Biological Chemistry and Molecular Pharmacology, Harvard Medical School, Bldg. C, Room 210, 240 Longwood Ave., Boston, MA 02115. Phone: (617) 432-0696. Fax: (617) 738-0516. E-mail: SteveB@hms.harvard.edu.

† Supplemental material for this article may be found at http://mcb.asm.org/.

‡ Present address: Department of Biochemistry, University of Oxford, Oxford OX1 3QU, United Kingdom.

▽ Published ahead of print on 27 June 2011.

affect the efficiency of termination by the Nrd1-Nab3-Sen1 pathway.

MATERIALS AND METHODS

Yeast strains and plasmids. *Saccharomyces cerevisiae* strains used in this study are listed in Table 1. Plasmid pJC643 was obtained from J. Corden (16), and plasmids pRS416-SET1(1-1080), pRS416-SET1(ΔRRM), and pRS416-SET1(780-1080) were obtained from S. Briggs (6, 18). A list of the oligonucleotides used is given in Table 2. The yeast plasmids expressing Set1 with an H422A or H1017K point mutation were made by inverse PCR of pRS416-SET1(1-1080) with primers Set1 H422A up and Set1 H422A down or with primers Set1 H1017K up and Set1 H1017K down.

Northern blotting. Northern blot experiments were performed as previously described (25, 59). Cultures grown overnight at room temperature were diluted and shifted to 30°C in the morning. The cultures were then grown until an optical density (OD) of 0.5 was reached and were harvested for RNA extraction. This temperature shift is especially important for experiments using *nrd1* partial deletion strains since they grow only very slowly at 30°C or higher for extended periods of time. A total of 5 to 20 μg of total RNA was resolved on 1.2% formaldehyde-agarose gels. PCR primers described in Table 2 were used to generate probes. The PCR-amplified DNA fragment was gel purified and labeled by using the Megaprime DNA labeling system (Amersham Bioscience).

ChIP. Chromatin immunoprecipitation (ChIP) experiments for tetra-acetylated H4 (catalog number 06-866; Upstate) and H3 (ab1791; Abcam) were performed as described previously (23, 26). Five micrograms of anti-Nrd1 antibody, kindly provided by J. Corden, was used per ChIP experiment. Monoclonal antibody against Rpb3 (1Y26; Neoclone) was used as previously described (1). All yeast strains were grown to an OD at 600 nm (OD_{600}) of ~0.5 in synthetic complete (SC) medium supplemented with 2% glucose. Primers for ChIP for *SNR13* were previously described (25). Twenty-six PCR cycles were used for anti-Rpb3, anti-Nrd1, anti-H3K4me3, anti-H3K4me2, and anti-H3 ChIPs. Anti-acetyl H4 ChIPs were analyzed by using 23 cycles to keep amplification in the linear range.

RT-PCR. One microgram of total RNA was used in a Superscript II reverse transcriptase (RT) (Invitrogen) reaction with gene-specific primers (Table 2). One-fiftieth of the cDNA was amplified by using the ChIP PCR protocol with various cycle numbers to achieve linear-range amplification (30 cycles for snoRNA read-through transcripts and CUTs, 20 cycles for full-length snoRNA, and 26 cycles for snR13 read-through transcripts). Note that the data were expressed by dividing the read-through signal by the total signal without correction for different cycle numbers. Therefore, these ratios are relative and not absolute measures of termination read-through. Quantitative PCR analyses to verify a key subset of RT-PCR results were performed by using 50-fold-diluted cDNA in a Roche Light Cycler 480 sequence detector with Eva-Green detection agent. In all cases, similar results were obtained with the two approaches.

NET-Seq. Native elongating transcript sequencing (NET-Seq) was performed with wild-type (WT) and *set1*Δ cells as previously described (14).

RESULTS

***SET1* interacts genetically with *NRD1*.** To test for a genetic interaction between *SET1* and *NRD1*, partial-deletion alleles of *NRD1* were combined with a *SET1* deletion, and the growth of the resulting double mutant cells was assayed by spotting onto plates and in liquid culture. The Nrd1 CID maps roughly to amino acids 1 to 150, while a region necessary and sufficient for the Nab3 interaction (Nab3 interaction domain [NID]) maps between residues 150 and 214 (16, 50, 60, 65) (Fig. 1A). The deletion of the CID [*nrd1*(*1–164*Δ) and *nrd1*(*6–150*Δ)] results in slightly slower growth than that of *NRD1* cells. However, the *nrd1*(*1–164*Δ) *set1*Δ and *nrd1*(*6–150*Δ) *set1*Δ double mutants showed a much slower growth phenotype than either the *nrd1*(*1–164*Δ) or *set1*Δ mutant alone (Fig. 1B and C). Since *nrd1*(*151–214*Δ) cells grew very poorly on plates at 30°C, we monitored growth in liquid culture. The doubling time of *nrd1*(*151–214*Δ) *set1*Δ cells was considerably longer than that observed for *nrd1*(*151–214*Δ) or *set1*Δ cells (Fig. 1C). This synthetic interaction suggests that Set1 might affect an Nrd1-dependent process.

***set1*Δ enhances the termination defect of *nrd1* mutants.** To test whether the observed genetic interaction between *SET1* and *NRD1* is due to a defect in termination, the expression of the *SNR13* gene was assayed by Northern blotting. In wild-type and *set1*Δ cells, transcription terminates within the downstream *TRS31* open reading frame (25, 52) (Fig. 2A, top). The terminated transcript is then trimmed to yield the mature snR13 transcript. For *nrd1*(*1–164*Δ) and *nrd1*(*151–214*Δ) cells, a larger dicistronic read-through transcript was also observed (Fig. 2A, bottom). The higher level of read-through transcripts in *nrd1*(*1–164*Δ) cells (Fig. 2A, bottom, compare lanes 3 and 5) is likely because the deletion of *nrd1*(*1–164*Δ) spans both the complete CID and part of the NID, while *nrd1*(*151–214*Δ) affects only Nab3 interactions. When *set1*Δ was deleted in either of the *nrd1* mutant strains, read-through transcript levels increased (Fig. 2A, bottom, and B). This effect is particularly striking with *nrd1*(*151–214*Δ). This result suggests that Set1 contributes to efficient Nrd1-dependent transcription termination.

To see if the termination effect of Set1 extends beyond Nrd1 mutant cells, we deleted *SET1* in a strain mutated for the Nrd1 partner Nab3. The *nab3-11* allele harbors two mutations in its RNA recognition motif (RRM) domain (16) and is defective in Nrd1-dependent transcription termination (51). RT-PCR analysis was performed for *nab3-11* and *nab3-11 set1*Δ cells grown at 30°C using primer sets against the body of snR13 and a downstream read-through region. A range of PCR cycle numbers and cDNA dilutions was tested to ensure linear-range amplification (data not shown and see Fig. S1A in the supplemental material). The deletion of *SET1* in a *nab3-11* mutant strain increased the accumulation of snR13 read-through transcripts (Fig. 2C), and this result was confirmed by quantitative real-time PCR (qPCR) (Fig. S1B).

The Nrd1-exosome pathway also mediates transcription termination and the degradation of cryptic unstable transcripts (CUTs), including several that emerge from heterochromatic regions of the genome (3, 52, 56, 61). Accordingly, Northern blot analysis of a CUT produced within the ribosomal DNA repeats (NTS1 CUT) was performed (Fig. 2D). No CUT accumulation was observed in wild-type or *set1*Δ cells. As expected, the cryptic transcript accumulated in *nrd1*(*1–164*Δ) and *nrd1*(*151–214*Δ) mutants (Fig. 2D, bottom). Consistent with the snR13 results, the levels of the CUT increased markedly when the *nrd1* mutants were combined with *set1*Δ.

We consistently observed that the *nrd1*(*1–164*Δ) mutant results in a stronger termination defect than the *nrd1*(*151–214*Δ) mutant at *SNR13* and the NTS1 CUT (Fig. 2A and D, compare lanes 3 and 5). This is likely because *nrd1*(*1–164*Δ) removes both the CTD binding domain and part of the Nab3 interaction domain, whereas the *nrd1*(*151–214*Δ) deletion abrogates only the interaction with Nab3 (Fig. 1A). Surprisingly, *nrd1*(*1–164*Δ) cells grow better than *nrd1*(*151–214*Δ) cells, suggesting that the severity of the growth phenotype could be due to defective termination affecting some essential gene where the Nab3 interaction is more important than CTD binding. Although *nrd1* mutants display different levels of read-through transcription, the deletion of *SET1* in either *nrd1* mutant background always results in increased levels of snR13 read-

TABLE 1. Yeast strains used in this study

Strain	Genotype	Reference (plasmid reference[s]) or source
YF336 (BY4741)	*mat***a** *ura3Δ0 leu2Δ0 his3Δ1 met15Δ0*	64
YF534	*mat***a** *ura3Δ0 leu2Δ0 his3Δ1 met15Δ0 rad6Δ::KanMX*	Saccharomyces Genome Deletion Project
YF688	*mat***a** *ura3Δ0 leu2Δ0 his3Δ1 met15Δ0 pho23Δ::KanMX*	Saccharomyces Genome Deletion Project
YF1557	*mat***a** *ura3Δ0 leu2Δ0 his3Δ1 met15Δ0 MUD2-TAP::HIS3*	Open Biosystems TAP-Fusion Library
YF1703	*mat***a** *ura3Δ0 leu2Δ0 his3Δ1 met15Δ0 rtr1Δ::KanMX*	Saccharomyces Genome Deletion Project
YF1495	*mat***a** *ura3Δ0 leu2Δ0 his3Δ1 met15Δ0 yng1Δ::KanMX*	Saccharomyces Genome Deletion Project
YF1471	*matα ura3-1 leu2-3,112 trp1-1 his3-11,15 ade2-1 can1-100 nab3-11*	16
YSB2086	*mat***a** *ura3-52 leu2-3,112 trp1-1 his3-11,15 lys2Δ2 ade2-1 met2Δ1 can1-100 nrd1Δ::HIS3* {pRS415-*nrd1*(*151-214Δ*) [*nrd1*(*151-214Δ*)-HA_2 *LEU2 CEN*]}	This study (61)
YSB2094	*mat***a** *ura3-52 leu2-3,112 trp1-1 his3-11,15 lys2Δ2 ade2-1 met2Δ1 can1-100 nrd1Δ::HIS3* {pJC643 [*nrd1(1-164Δ)*-HA_2 *LEU2 CEN*]}	60 (16)
YSB2152	*mat***a** *ura3-52 leu2-3,112 trp1-1 his3-11,15 lys2Δ2 ade2-1 met2Δ1 can1-100 nrd1Δ::HIS3 set1Δ::KanMX* {pRS415-*nrd1*(*151-214Δ*) [*nrd1*(*151-214Δ*)-HA_2 *LEU2 CEN*]}	This study (61)
YSB2153	*mat***a** *ura3-52 leu2-3,112 trp1-1 his3-11,15 lys2Δ2 ade2-1 met2Δ1 can1-100 nrd1Δ::HIS3 set1Δ::KanMX* {pJC643 [*nrd1*(*1-164Δ*)-HA_2 *LEU2 CEN*]}	This study (16)
YSB2253	*mat***a** *ura3Δ0 leu2Δ0 his3Δ1 met15Δ0 set1Δ::HISMX6*	T. Kim
YSB2256	*mat***a** *ura3-52 leu2Δ1 trp1Δ63 his3Δ200 lys2-801 ade2-101 hht1-hhf1*::pWZ405-*F2F9-LEU2 hht2-hhf2*::pWZ403-*F4F10-HIS3* {pJH18-*H3-H4-WT* [*HHT2* (histone H3) *HHF2* (histone H4) *TRP1 CEN*]}	T. Kim (5)
YSB2257	*mat***a** *ura3-52 leu2Δ1 trp1Δ63 his3Δ200 lys2-801 ade2-101 hht1-hhf1*::pWZ405-*F2F9-LEU2 hht2-hhf2*::pWZ403-*F4F10-HIS3* {pRS314-*H3*(*K4R*)*/H4* [*hht2* (*K4R*) (histone H3) *HHF2* (histone H4) *TRP1 CEN*]}	T. Kim (plasmid, M. Keogh)
YSB2325	*mat***a** *ura3Δ0 leu2Δ0 his3Δ1 met15Δ0 MUD2-TAP::HIS3 rad6Δ::KanMX*	This study
YSB2409	*mat***a** *ura3-52 leu2-3,112 trp1-1 his3-11,15 lys2Δ2 ade2-1 met2Δ1 can1-100 nrd1Δ::HIS3 pho23Δ::KanMX* {pJC643 [*nrd1*(*1-164Δ*)-HA_2 *LEU2 CEN*]}	This study (16)
YSB2412	*mat***a** *ura3-52 leu2-3,112 trp1-1 his3-11,15 lys2Δ2 ade2-1 met2Δ1 can1-100 nrd1Δ::HIS3 pho23Δ::KanMX* {pRS415-*nrd1*(*151-214Δ*) [*nrd1*(*151-214Δ*)-HA_2 *LEU2 CEN*]}	This study (61)
YSB2415	*mat***a** *ura3-52 leu2-3,112 trp1-1 his3-11,15 lys2Δ2 ade2-1 met2Δ1 can1-100 nrd1Δ::HIS3 rad6Δ::KanMX* {pJC643 [*nrd1*(*1-164Δ*)-HA_2 *LEU2 CEN*]}	This study (16)
YSB2420	*mat***a** *ura3-52 leu2-3,112 trp1-1 his3-11,15 lys2Δ2 ade2-1 met2Δ1 can1-100 nrd1Δ::HIS3 pho23Δ::KanMX set1Δ::TRP1* {pRS415-*nrd1*(*151-214Δ*) [*nrd1*(*151-214Δ*)-HA_2 *LEU2 CEN*]}	This study (61)
YSB2421	*mat***a** *ura3-52 leu2-3,112 trp1-1 his3-11,15 lys2Δ2 ade2-1 met2Δ1 can1-100 nrd1Δ::HIS3 pho23Δ::KanMX set1Δ::TRP1* {pJC643 [*nrd1*(*1-164Δ*)-HA_2 *LEU2 CEN*]}	This study (16)
YSB2488	*mat***a** *ura3-52 leu2-3,112 trp1-1 his3-11,15 lys2Δ2 ade2-1 met2Δ1 can1-100 nrd1Δ::HIS3 rtr1Δ::KanMX* {pRS415-*nrd1*(*151-214Δ*) [*nrd1*(*151-214Δ*)-HA_2 *LEU2 CEN*]}	This study (61)
YSB2489	*mat***a** *ura3-52 leu2-3,112 trp1-1 his3-11,15 lys2Δ2 ade2-1 met2Δ1 can1-100 nrd1Δ::HIS3 yng1Δ::KanMX* {pRS415-*nrd1*(*151-214Δ*) [*nrd1*(*151-214Δ*)-HA_2 *LEU2 CEN*]}	This study (61)
YSB2491	*mat***a** *ura3-52 leu2-3,112 trp1-1 his3-11,15 lys2Δ2 ade2-1 met2Δ1 can1-100 nrd1Δ::HIS3 set1Δ::KanMX rtr1Δ::NATMX* {pRS415-*nrd1*(*151-214Δ*) [*nrd1*(*151-214Δ*)-HA_2 *LEU2 CEN*]}	This study (61)
YSB2492	*mat***a** *ura3-52 leu2-3,112 trp1-1 his3-11,15 lys2Δ2 ade2-1 met2Δ1 can1-100 nrd1Δ::HIS3 pho23Δ::KanMX yng1Δ::NATMX* {pRS415-*nrd1*(*151-214Δ*) [*nrd1*(*151-214Δ*)-HA_2 *LEU2 CEN*]}	This study (61)
YSB2502	*mat***a** *ura3-52 leu2-3,112 trp1-1 his3-11,15 lys2Δ2 ade2-1 met2Δ1 can1-100 nrd1Δ::HIS3 set1Δ::KanMX* {pRS415-*nrd1*(*151-214Δ*) [*nrd1*(*151-214Δ*)-HA_2 *LEU2 CEN* pRS416-*SET1*(*1-1080*) (*Flag-SET1 URA3 CEN*)]}	This study (18, 61)
YSB2503	*mat***a** *ura3-52 leu2-3,112 trp1-1 his3-11,15 lys2Δ2 ade2-1 met2Δ1 can1-100 nrd1Δ::HIS3 set1Δ::KanMX* {pRS415-*nrd1*(*151-214Δ*) [*nrd1*(*151-214Δ*)-HA_2 *LEU2 CEN* pRS416-*SET1*(*ΔRRM*) [*Flag-SET1*(*230-335Δ*) *URA3 CEN*]}	This study (18, 61)
YSB2504	*mat***a** *ura3-52 leu2-3,112 trp1-1 his3-11,15 lys2Δ2 ade2-1 met2Δ1 can1-100 nrd1Δ::HIS3 set1Δ::KanMX* {pRS415-*nrd1*(*151-214Δ*) [*nrd1*(*151-214Δ*)-HA_2 *LEU2 CEN*] pRS416-*SET1*(*780-1080*) [*Flag-SET1*(*1-779Δ*) *URA3 CEN*]}	This study (18, 61)
YSB2505	*mat***a** *ura3-52 leu2-3,112 trp1-1 his3-11,15 lys2Δ2 ade2-1 met2Δ1 can1-100 nrd1Δ::HIS3 set1Δ::KanMX* {pRS415-*nrd1*(*151-214Δ*) [*nrd1*(*151-214Δ*)-HA_2 *LEU2 CEN* pRS416-*set1*(*H422A*) [*Flag-set1*(*H422A*) *URA3 CEN*]}	This study (61)
YSB2506	*mat***a** *ura3-52 leu2-3,112 trp1-1 his3-11,15 lys2Δ2 ade2-1 met2Δ1 can1-100 nrd1Δ::HIS3 set1Δ::KanMX* {pRS415-*nrd1*(*151-214Δ*) [*nrd1*(*151-214Δ*)-HA_2 *LEU2 CEN* pRS416-*set1*(*H1017K*) [*Flag-set1*(*H1017K*) *URA3 CEN*]}	This study (61)

Continued on following page

TABLE 1—*Continued*

Strain	Genotype	Reference (plasmid reference[s]) or source
YSB2507	*mat***a** *ura3-52 leu2-3,112 trp1-1 his3-11,15 lys2Δ2 ade2-1 met2Δ1 can1-100 nrd1Δ::HIS3 set1Δ::KanMX* {pJC643 [*nrd1*(*1-164Δ*)-*HA*$_2$ *LEU2 CEN*] pRS416-*SET1*(*1-1080*) (*Flag-SET1 URA3 CEN*)}	This study (16, 18)
YSB2508	*mat***a** *ura3-52 leu2-3,112 trp1-1 his3-11,15 lys2Δ2 ade2-1 met2Δ1 can1-100 nrd1Δ::HIS3 set1Δ::KanMX* {pJC643 [*nrd1*(*1-164Δ*)-*HA*$_2$ *LEU CEN*] pRS416-*SET1*(*ΔRRM*) [*Flag-SET1*(*230-335Δ*) *URA3 CEN*]}	This study (16, 18)
YSB2509	*mat***a** *ura3-52 leu2-3,112 trp1-1 his3-11,15 lys2Δ2 ade2-1 met2Δ1 can1-100 nrd1Δ::HIS3 set1Δ::KanMX* {pJC643 [*nrd1*(*1-164Δ*)-*HA*$_2$ *LEU2 CEN*] pRS416-*SET1*(*780-1080*) [*Flag-SET1*(*1-779Δ*) *URA3 CEN*]}	This study (16, 18)
YSB2510	*mat***a** *ura3-52 leu2-3,112 trp1-1 his3-11,15 lys2Δ2 ade2-1 met2Δ1 can1-100 nrd1Δ::HIS3 set1Δ::KanMX* {pJC643 [*nrd1*(*1-164Δ*)-*HA*$_2$ *LEU2 CEN*] pRS416-*set1*(*H422A*) [*Flag-set1*(*H422A*) *URA3 CEN*]}	This study (16)
YSB2511	*mat***a** *ura3-52 leu2-3,112 trp1-1 his3-11,15 lys2Δ2 ade2-1 met2Δ1 can1-100 nrd1Δ::HIS3 set1Δ::KanMX* {pJC643 [*nrd1*(*1-164Δ*)-*HA*$_2$ *LEU2 CEN*] pRS416-*set1*(*H1017K*) [*Flag-set1*(*H1017K*) *URA3 CEN*]}	This study (16)
YSB2559	*matα ura3-1 leu2-3,112 trp1-1 his3-11,15 ade2-1 can1-100 nab3-11 set1Δ::TRP1*	This study
YSB2397	*mat***a** *ura3-52 leu2Δ1 trp1Δ63 his3Δ200 lys2-128δ rrp6Δ::KanMX*	This study
YSB2398	*mat***a** *ura3-52 leu2Δ1 trp1Δ63 his3Δ200 lys2-128δ set1Δ::HISMX6 rrp6Δ::KanMX*	This study
YSB2582	*matα ura3-52 leu2-3,112 his3Δ200 set1Δ::KanMX nrd1Δ::HIS3* {pRS415-*nrd1*(*151-214*) [*nrd1*(*151-214Δ*)-*HA*$_2$ *LEU2 CEN*]}	This study (61)
YSB2583	*matα ura3-52 leu2-3,112 his3Δ200 set1Δ::KanMX nrd1Δ::HIS3* {pRS415-*nrd1*(*151-214Δ*) [*nrd1*(*151-214Δ*)-*HA*$_2$ *LEU2 CEN*] *rpb2-10* [*rpb2-10*(*P1018S*) *URA3*]}	This study (45, 61)
YSB2574	*matα ura3-52 leu2-3,112 his3Δ200 pho23Δ::NATMX nrd1Δ::KanMX* {pRS415-*nrd1*(*151-214Δ*) [*nrd1*(*151-214Δ*)-*HA*$_2$ *LEU2 CEN*]}	This study (61)
YSB2595	*matα ura3-52 leu2-3,112 his3Δ200 pho23Δ::NATMX nrd1Δ::KanMX* {pRS415-*nrd1*(*151-214Δ*) [*nrd1*(*151-214Δ*)-*HA*$_2$ *LEU2 CEN rpb2-10* [*rpb2-10*(*P1018S*) *URA3*]}	This study (45, 61)
YSB2064	*mat***a** *ura3Δ0 leu2Δ0 his3Δ1 met15Δ0 nrd16-150Δ*	60
YSB2665	*mat***a** *ura3Δ0 leu2Δ0 his3Δ1 met15Δ0 nrd16-150Δ set1Δ::KanMX*	This study

through or NTS1 CUT transcripts (Fig. 2A and D, compare lanes 4 and 6).

H3K4 trimethylation contributes to Nrd1-dependent termination. Set1 has two predicted RRM domains in its N-terminal region, the second of which exhibits RNA binding activity *in vitro* (58). The *in vivo* relevance of this activity remains to be elucidated. The C-terminal half of Set1 contains a histone methyltransferase SET domain (6, 18, 46, 58). To determine which domains and functions of Set1 are required to support Nrd1-dependent termination, various *set1* mutants (Fig. 3A) were combined with the *nrd1*(*1–164*Δ) mutation and tested for synthetic growth phenotypes. The deletion of RRM1 [*set1*(*230–335*Δ)] or both RRMs [*set1*(*1–779*Δ)] disrupts H3K4 trimethylation (H3K4me3) but not dimethylation or monomethylation (18, 26, 46). These Set1 deletion mutants resulted in the same enhancement of the *nrd1* mutant growth and termination defect as that of *set1*Δ (Fig. 3B to D), suggesting that H3K4me3 is the histone modification that is relevant for efficient snoRNA termination.

To test whether the genetic interaction between *NRD1* and *SET1* is dependent on the SET domain or RNA binding activities of Set1, two point mutants of Set1 were assayed for termination defects. The *set1*(*H422A*) mutation abolishes RNA binding *in vitro* without affecting *in vivo* histone methylation levels (see Fig. S2 in the supplemental material) (58). In contrast, the *set1*(*H1017K*) catalytic-site mutation eliminates H3K4 methylation activity *in vivo* (46). The *set1*(*H422A*) mutant showed no additional growth defect when combined with an *nrd1* mutant (Fig. 3B). In contrast, the active-site mutant showed the same growth defect enhancement as that of *set1*Δ. In agreement with the growth phenotypes, snR13 read-through transcript and NTS1 CUT levels increased when an *nrd1* mutant was combined with *set1*(*H1017K*) or *set1*(*230–335*Δ) (Fig. 3C and D). In contrast, *set1*(*H422A*) caused little or no additional accumulation of these transcripts.

The monoubiquitylation of histone H2B K123 by the Rad6-Bre1 complex is important for higher levels of methylation of H3K4 by Set1 (53). In *rad6*Δ cells, di- and trimethylation of H3K4 are lost, while monomethylation is intact (29). The combination of *rad6*Δ with a *nrd1* mutation increased the read-through transcription of snR13 (Fig. 3E). Confirming the connection between Nrd1 and H2B K123 ubiquitylation, it was recently reported that a low level of increased snoRNA read-through was seen in *rad6*Δ, *bre1*Δ, or H2BK123R mutant cells (57). Similarly, an increased accumulation of snR13 read-through transcripts was observed for a wild-type *NRD1* strain carrying an H3K4R mutation (Fig. 3F), supporting the significance of H3K4 methylation. Taken together, these results indicate that Set1 and H3K4 trimethylation are important for efficient Nrd1-dependent termination, while Set1 RNA binding is not.

Nrd1 recruitment is reduced in *set1*Δ cells. Nrd1 can be recruited to target genes via its RNA binding domain, via its CTD interaction, or via its interaction with Nab3. Because Nrd1 termination defects correlate closely with reduced recruitment, we compared the chromatin immunoprecipitation (ChIP) signals of Nrd1 in *nrd1*(*151–214*Δ) and *nrd1*(*151–214*Δ) *set1*Δ cells (Fig. 4B). Nrd1 cross-links to the *SNR13* transcribed region (PCR products 2 and 3) (Fig. 4A and B). The Nrd1

TABLE 2. Oligonucleotides used in this study

Oligonucleotide	Oligonucleotide ID	Sequence (5′–3′)	Purpose(s)
snR13 1 up	1309	TTATAAATGGCATCTCAAATCGTC	ChIP, Northern probe
snR13 1 down	1310	GGTCAGATAAAAGTAAAAAAAGGTAGC	ChIP, Northern probe, RT-PCR
snR13 1 top	2435	CCTTTTTATATGATGAATATGAGTGC	RT-PCR
snR13 2 up	1311	CTGACCTTTTAACTTCCCCGTAG	ChIP, RT-PCR
snR13 2 down	1312	CTGTCGCTTCCGTGTCTCTTGTCCTG	ChIP, RT-PCR
snR13 3 up	1313	CACGGAAGCGACAGAAAGACAGGGAG	ChIP
snR13 3 down	1314	CTAGAGGGAATGTATGTTGTTGAAG	ChIP
snR13 4 up	1315	GAGCATCTGCTTTCCTTTCAC	ChIP
snR13 4 down	1316	ATCACGGCGCCTCATCTTTG	ChIP
snR13 5 up	1317	AAAACCAAGAAAAGGATAAAGAG	ChIP
snR13 5 down	1318	TCGGTGTCTACAAAATGATACGC	ChIP
Pho23 up	1447	GATCCGCCTCTTCGCCCAGCAC	Amplify deletion cassette
Pho23 down	1448	CACACCACCCACTGTACGGCGATTAG	Amplify deletion cassette
Rad6 up	1449	AGCAACCATGAAACACTATATTCG	Amplify deletion cassette
Rad6 down	1450	ACGGCGAGCTTGGTGTCATTATG	Amplify deletion cassette
Set1 up	1695	GTATTATATAAAATCGATGTCGCATTAGTC	Amplify deletion cassette
Set1 down	1696	CCATCAAGTCACGAACATATTGTAATG	Amplify deletion cassette
rDNA #14 up	1707	CCGGGGCCTAGTTTAGAGAG	Northern probe
rDNA #15 down	1710	TCCCCACTGTTCACTGTTCA	Northern probe
Yng1 up	2254	GGCGCTCGACCCTCTCC	Amplify deletion cassette
Yng1 down	2255	CATCATGGTTAAAGGTTGTATCCC	Amplify deletion cassette
Rtr1 up	2256	CAGAAGTGGTCAAAAGCAATGG	Amplify deletion cassette
Rtr1 down	2257	GAACCAAAACTCTGAAGCAACACT	Amplify deletion cassette
Set1 H422A up	2096	ATAACAGACCTGTTTTAGCTGTCTCCAAAATATTTGTTG	Introduce H422A mutation
Set1 H422A down	2097	CAACAAATATTTTGGAGACAGCTAAAACAGGTCTGTTAT	Introduce H422A mutation
Set1 H1017K up	2098	TAGCCCGTTTCATTAATAAATGTTGTGATCCAAATTGTAC	Introduce H1017K mutation
Set1 H1017K down	2099	GTACAATTTGGATCACAACATTTATTAATGAAACGGGCTA	Introduce H1017K mutation
snR3 1 up	2353	GTACTAATCCACCGCATTAGACAGT	RT-PCR
snR3 1 down	2354	CTTCTGACACTCGAGTCTCATTCA	RT-PCR
snR3 2 up	2355	ATCCGTATGGGTGCAATCAAAG	RT-PCR
snR3 2 down	2356	CGAGTGTCTGGCCGAATGTC	RT-PCR
snR9 1 up	2357	GAACTTTCTACGCCTTTTCCTCTATG	RT-PCR
snR9 1 down	2358	GTCTGAAGGACTAATGATAGGTGGG	RT-PCR
snR9 2 up	2359	AAGCTTTCTTAACTCTTGCATCACTAC	RT-PCR
snR9 2 down	2360	CGATATAGGGCAGAACAAGGAGT	RT-PCR
snR71 1 up	2361	GATGATAACCTTCTCAGCTCACTCA	RT-PCR
snR71 1 down	2362	GGTCAGATAAATTGATGAATGTTGG	RT-PCR
snR71 2 up	2363	ATCTTACATGAAACTTAAACACGATACAT	RT-PCR
snR71 2 down	2364	CACGGCCTGTACACGAACTAT	RT-PCR
snR190 1 up	2365	GGCCCTGATGATAATGGTGTCT	RT-PCR
snR190 1 down	2366	GGCTCAGATCTGCATGTGTTGTAT	RT-PCR
snR128 1 up	2367	GATCACGGTGATGAAAGACTGG	RT-PCR
snR128 1 down	2368	CTACAGTATACGATCACTCAGACATCCTA	RT-PCR
snR128 2 up	2369	CTTTATCAAACCAGCTTACCAACATT	RT-PCR
snR128 2 down	2370	TGGTCAAAGGAATCGAACAAGA	RT-PCR
FMP40 up	2347	GGTTGAAGTTACCCAAGCGGATCC	RT-PCR, ChIP
FMP40 down	2348	CAATTCGGCTCATTTGCTGCACAGC	RT-PCR, ChIP
RPR2 up	2351	GACTCGAGCTCAGTGAGCCGTTTATTATTAC	RT-PCR
RPR2 down	2352	GCCATCAGAGGGTTAGAAACACCTATTGTAAG	RT-PCR
NEL025C up	2349	GTAGTCGCCAACAATCATTTCGATACAACTTG	RT-PCR, ChIP
NEL025C down	2350	CAACCGCTGTTGTCAAACAAGACTATAGG	RT-PCR, ChIP

ChIP signal was reduced when *set1*Δ was combined with the *nrd1* mutant. This reduction was not due to changes in overall Nrd1 protein levels (Fig. 4C). ChIP of Rpb3 showed that reduced Pol II recruitment was also not responsible for the reduced Nrd1 cross-linking (Fig. 4D). Indeed, a slight increase in Rpb3 recruitment further downstream of *SNR13* (PCR products 3 to 5) was observed for *nrd1*(*151–214*Δ) *set1*Δ cells, as expected due to increased termination readthrough (Fig. 2A).

The effects of Set1 RRM deletions on snR13 and NTS1 CUT read-through (Fig. 3) suggest that H3K4 trimethylation contributes specifically to Nrd1-dependent termination. Therefore, Nrd1 recruitment was assayed in *nrd1*(*151–214*Δ) *set1*(*230–335*Δ) double mutant cells. As with *set1*Δ, the combination of *set1*(*230–335*Δ) with the *nrd1* mutant decreased the recruitment of Nrd1 to *SNR13* (Fig. 4B; for Rpb3 levels see Fig. 4D). Since *set1*(*230–335*Δ) specifically abolishes H3K4 trimethylation while leaving di- and monomethylation intact, these results suggest that it is H3K4 trimethylation that enhances Nrd1 recruitment to chromatin.

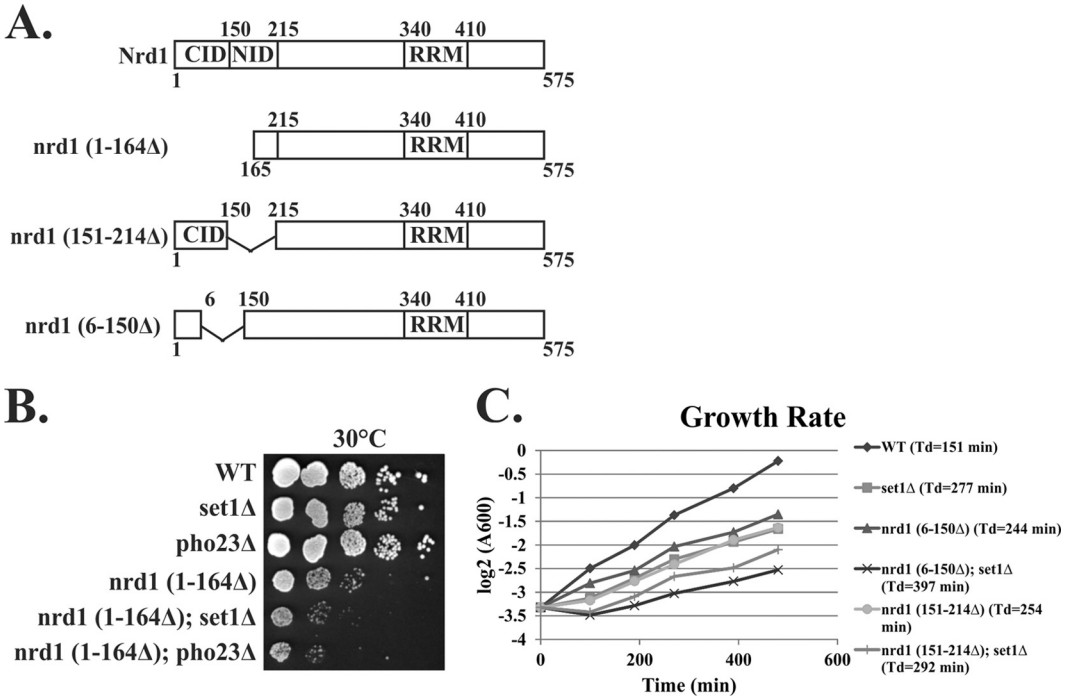


FIG. 1. *SET1* interacts genetically with *NRD1*. (A) Schematic representation of the Nrd1 domain structure and deletion mutants. Annotated are the CTD interaction domain (CID), the Nab3 interaction domain (NID), and the RNA recognition motif (RRM). (B) Growth of the WT (BY4741), *set1*Δ (YSB2253), *pho23*Δ (YF688), *nrd1*(*1–164*Δ) (YSB2094), *nrd1*(*1–164*Δ) *set1*Δ (YSB2153), and *nrd1*(*1–164*Δ) *pho23*Δ (YSB2409) strains. Strains were plated with 10-fold serial dilutions on synthetic complete (SC) medium and incubated for 2 days at 30°C. (C) Growth curves of WT (BY4741), *set1*Δ, *nrd1*(*151–214*Δ), *nrd1*(*6–150*Δ), *nrd1*(*151–214*Δ) *set1*Δ, *and nrd1*(*6–150*Δ) *set1*Δ strains assayed in liquid synthetic complete medium at 30°C starting from an A_{600} of 0.1. For strain information see Table 1. The graph key shows the calculated doubling time (Td) of each strain in parentheses.

Proper levels of histone acetylation promote Nrd1-dependent termination. We hypothesized that protein complexes that recognize H3K4 methylation might mediate the effects of Set1 on Nrd1-dependent termination. A previous large-scale genetic interaction study (15) showed that deletions of *PHO23* or other members of the Rpd3L (Rpd3 large) HDAC complex cause synthetic slow growth in combination with a hypomorphic *nrd1* mutant allele. We confirmed a strong genetic interaction between *pho23*Δ and *nrd1*(*1–164*Δ) (Fig. 1B). Rpd3L is typically thought of as a corepressor that is recruited to a small set of promoters by sequence-specific binding partners. However, Rpd3L contains two PHD finger proteins, Pho23 and Cti6, that preferentially bind H3K4-methylated histone tail peptides *in vitro* (49). Therefore, we considered Rpd3L as a candidate for affecting Nrd1-dependent termination.

RNA analysis showed that *pho23*Δ increased snR13 read-through in *nrd1*(*151–214*Δ) cells (Fig. 5A, compare lanes 4 and 5). We also quantitated the termination defect of *set1*Δ and *pho23*Δ in the *nrd1*(*151–214*Δ) background using RT-PCR (Fig. 5F) and quantitative real-time PCR (see Fig. S1C in the supplemental material). These results confirm the effects that we observed by Northern blot analyses. It should be noted that the Northern blots show the stable, polyadenylated snR13-TRS31 read-through transcript. However, in RT-PCR experiments, we were able to include the quantitation of transcripts that correspond to all Pol II termination events prior to the downstream TRS31 termination site, including rapidly degraded, nonpolyadenylated species. Therefore, small termination defects in *set1*Δ and *pho23*Δ cells that were below the detection limit of the Northern blots were observable (Fig. 6).

To test whether the Rpd3L HDAC affects *SNR13* chromatin, levels of histone H4 acetylation in WT and *pho23*Δ cells were analyzed (Fig. 5B). Despite the fact that *SNR13* is transcriptionally very active and not known to be a target for Rpd3L, a small increase in H4 acetylation levels was reproducibly observed at the *SNR13* promoter in *pho23*Δ cells. In agreement with a direct effect, a ChIP with microarray technology (ChIP-chip) trace for the histone deacetylase Rpd3 showed enrichment over the snR13 region (Fig. 5C) (data from reference 7).

If increased histone acetylation underlies the enhancement of the *nrd1* mutant termination defect by *pho23*Δ, we reasoned that the deletion of an opposing histone acetyltransferase (HAT) might suppress the *pho23*Δ read-through phenotype. The NuA3 HAT complex is recruited to promoter regions, at least in part by its subunit Yng1, a PHD finger protein that specifically binds H3K4me3 (19, 32, 35, 55). The deletion of *YNG1* reduced the termination defect at *SNR13* observed for *nrd1*(*151–214*Δ) *pho23*Δ cells (Fig. 5D). This suppression suggests a model in which H3K4 trimethylation targets both NuA3 and Rpd3L complexes to *SNR13* via Yng1 and Pho23, respectively. The proper balance of acetylation and deacetylation might affect early elongation and thereby influence the Nrd1 early termination pathway. Accordingly, H4 acetylation levels were decreased at *SNR13* in *yng1*Δ cells (Fig. 5E). This model can also explain why read-through in the *nrd1*(*151–214*Δ) *pho23*Δ strain is greater than that seen for *nrd1*(*151–214*Δ)

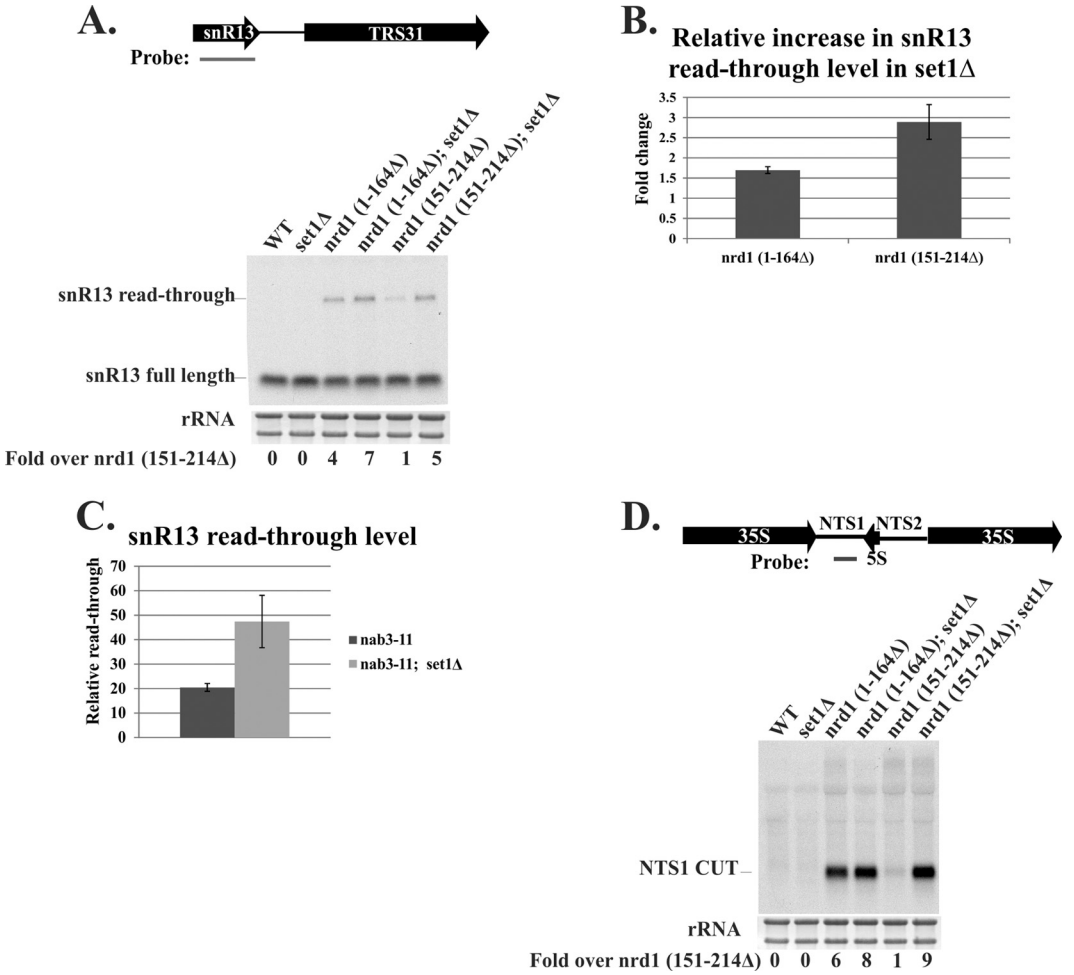


FIG. 2. Deletion of *SET1* enhances the termination defect of *nrd1* and *nab3* mutants. (A, top) Schematic representation of the *SNR13* region. *SNR13* is upstream of the infrequently transcribed *TRS31* gene. The probe used for hybridization is indicated by the horizontal bar below the schematic. (Bottom) Total RNA (5 μg) from WT (BY4741), *set1*Δ (YSB2253), *nrd1*(*1–164*Δ) (YSB2094), *nrd1*(*1–164*Δ) *set1*Δ (YSB2153), *nrd1*(*151–214*Δ) (YSB2086), and *nrd1*(*151–214*Δ) *set1*Δ (YSB2152) strains was analyzed by Northern blot using the *SNR13* probe. The positions of mature full-length snR13 and stable snR13-TRS31 read-through RNAs are marked on the left. The bottom shows methylene blue staining of 25S and 18S rRNAs as a loading control. Transcripts were quantitated with a phosphorimager. snR13 read-through transcripts were calculated as a percentage of full-length snR13. These numbers were divided by the value for the *nrd1*(*151–214*Δ) strain to give the "fold over *nrd1*(*151–214*Δ)" values listed below each lane. (B) Effect of *set1*Δ on the snR13 read-through transcript levels in *nrd1*(*1–164*Δ) and *nrd1*(*151–214*Δ) mutants quantified as the ratio of the *nrd1 set1* double mutant to the *nrd1* mutant alone using values from at least four Northern blot experiments. Error bars show standard deviations. (C) RT-PCR of snR13 read-through (26 cycles, using primers downstream of the normal termination site) and total (full-length plus read-through) transcripts (20 cycles, using primers within the mature snR13) were performed on RNA from three independent cultures of *nab3-11* (YF1471) and *nab3-11 set1*Δ (YSB2559) strains grown at the semipermissive temperature of 30°C. Quantitation by phosphorimager analysis is expressed by dividing the read-through by the total signal. Because these ratios were not corrected for numbers of PCR cycles, they are a relative, not absolute, measure of the read-through. This experiment was repeated by using RT-qPCR, which gave similar results (see Fig. S1B in the supplemental material). (D, top) Schematic representation of the rDNA region. 35S rRNA genes are interspersed with nontranscribed spacer 1 (NTS1), the 5S rRNA gene (black arrow), and nontranscribed spacer 2 (NTS2). The position of the probe used to detect the NTS1 CUT is shown below the diagram as a black line. (Bottom) RNA samples as in panel A were analyzed by Northern blotting using the NTS1 CUT probe. Levels of the NTS1 CUT were normalized to the methylene blue 25S rRNA signal. These values for each strain were then divided by the value of the *nrd1*(*151–214*Δ) strain to give the "fold over *nrd1*(*151–214*Δ)" values that are listed below each lane.

*set1*Δ cells (Fig. 5A, compare lanes 4 to 6). Whereas *pho23*Δ would reduce the recruitment of the HDAC Rpd3L, the deletion of *SET1* would lead to the loss of both the HDAC and the antagonistic HAT complex. Therefore, the increase in histone acetylation levels is less broad and pronounced in *set1*Δ cells than in *pho23*Δ cells (Fig. 5E).

Set1 and Pho23 affect termination of other snoRNAs and CUTs. To extend our results beyond *SNR13*, several other snoRNAs and CUTs were analyzed. Interestingly, while the deletion of *SET1* strongly increased the levels of the ribosomal DNA (rDNA) NTS1 CUT in *nrd1*(*151–214*Δ) cells, no such enhancement was seen with the deletion of *PHO23* (Fig. 5G). In fact, *pho23*Δ in *nrd1*(*151–214*Δ) *set1*Δ cells actually reduced the accumulation of the NTS1 CUT to nearly WT levels. These results may be due to the fact that repression within the rDNA heterochromatin is maintained by the Sir2 HDAC rather than

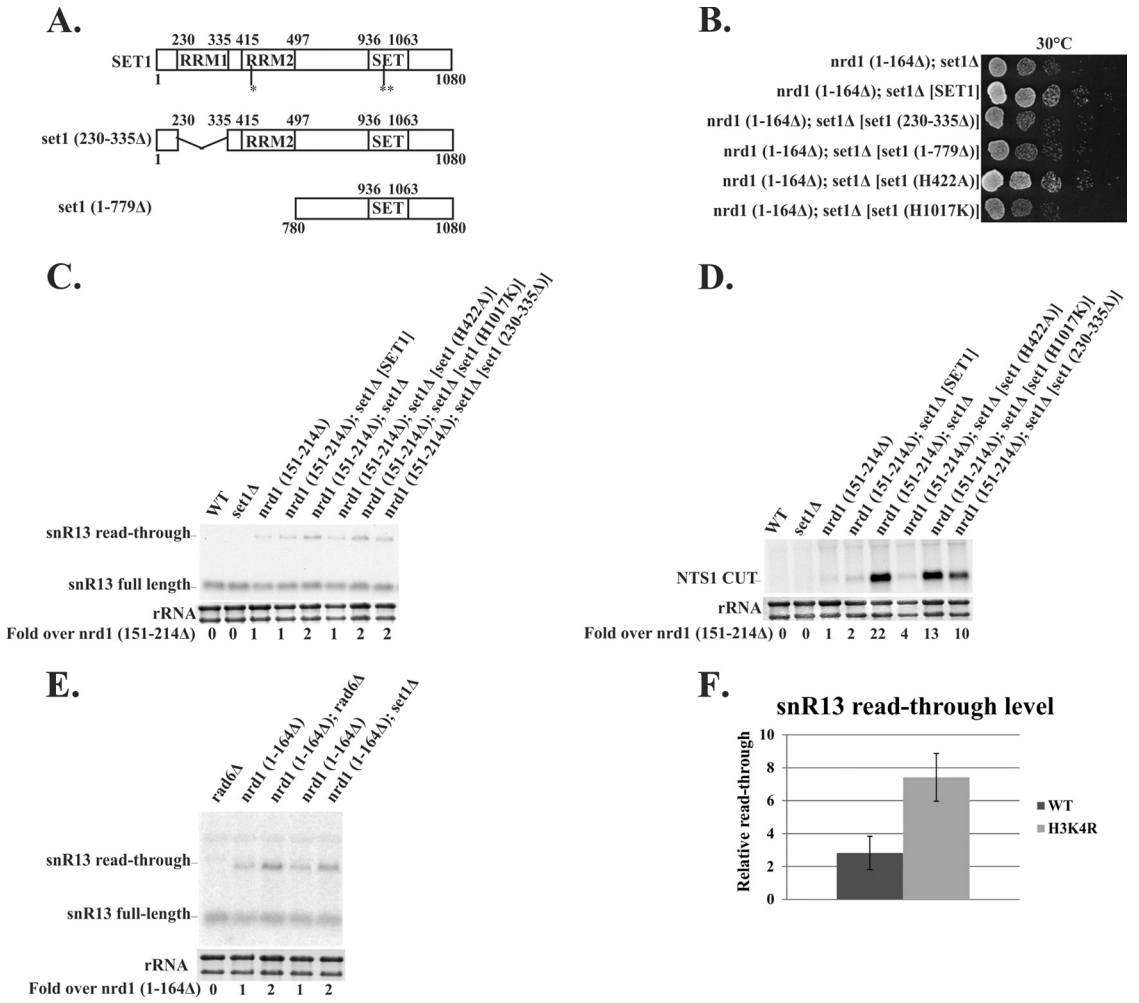


FIG. 3. Effect of Set1 on Nrd1-dependent termination is dependent on H3K4me3. (A) Schematic representation of the Set1 domain structure and mutants used in this study. Set1 has two predicted RNA recognition motifs (RRM1 and RRM2) in its N-terminal region. A SET domain in the C-terminal region is responsible for the methyltransferase activity of Set1. The single asterisk represents the position of the H422A point mutant that abolishes the *in vitro* RNA binding activity of Set1. The double asterisk shows the H1017K mutation in the methyltransferase active site of Set1. (B) An *nrd1*(*1–164*Δ) *set1*Δ strain (YSB2153) was transformed with the indicated plasmids expressing WT or mutant Set1 (the *SET1* allele on the plasmid is shown in square brackets) (for strain names and full genotypes see YSB2507 to YSB2511 in Table 1). The growth of the strains was assayed by 10-fold serial dilutions on synthetic complete medium plates lacking uracil at 30°C for 2 days. (C) Northern blot analysis of total RNA (5 μg) extracted from strains BY4741, YSB2253, YSB2086, YSB2502, YSB2152, YSB2505, YSB2506, and YSB2503. The plasmid-borne *SET1* alleles transformed into *nrd1*(*1–164*Δ) *set1*Δ cells are shown in square brackets. The positions of mature full-length snR13 and snR13-TRS31 read-through transcripts are indicated on the left. The methylene blue staining of 25S and 18S rRNAs as a loading control is shown at the bottom. The numbers below the gels show the quantitation of the snR13 read-through transcript level as fold over *nrd1*(*151–214*Δ) as described in the legend of Fig. 2A. (D) Northern blot analysis as in C except with the blot probed for the NTS1 CUT. (E) Northern blot analysis as in panel C using total RNA (5 μg) extracted from strains YF534, YSB2094, YSB2415, and YSB2153. (F) RT-PCR of snR13 read-through transcripts (31 cycles) and total (full-length plus read-through) transcripts (20 cycles) performed by using three independent cultures of WT (YSB2256) and H3K4R (YSB2257) strains grown at 30°C.

an Rpd3 complex. Indeed, consistent with our findings, previous studies showed that the deletion of Rpd3L complex members enhanced heterochromatic silencing (33, 54).

We assayed the termination of four additional snoRNAs and three CUTs by reverse transcription and PCR. The deletion of either *SET1* or *PHO23* in the *nrd1*(*151–214*Δ) background resulted in the increased read-through transcription of snR128 (Fig. 6A). The direct involvement of the Rpd3L complex is supported by the strong cross-linking of Rpd3 to this region (7) (see Fig. S3A in the supplemental material). Using this more sensitive RT-PCR assay, we also noted a slight increase in levels of read-through transcripts in *set1*Δ or *pho23*Δ cells, even in the wild-type *NRD1* background. Termination defects caused by *set1*Δ or *pho23*Δ were also seen for snR3, snR71, snR9, and the *RPR2* CUT (Fig. 6C and D). Interestingly, the *NEL025C* and *FMP40* CUT levels were increased by the deletion of *SET1* but not *PHO23* (Fig. 6B and D). In agreement with this, H4 acetylation levels were unaffected by *pho23*Δ in these regions (Fig. S3B). Similarly, no Rpd3 recruitment to the *NEL025C* CUT region was observed (Fig. S3C). It is possible that other HAT or HDAC complexes determine acetylation levels at these promoters. These results suggest that Set1 gen-

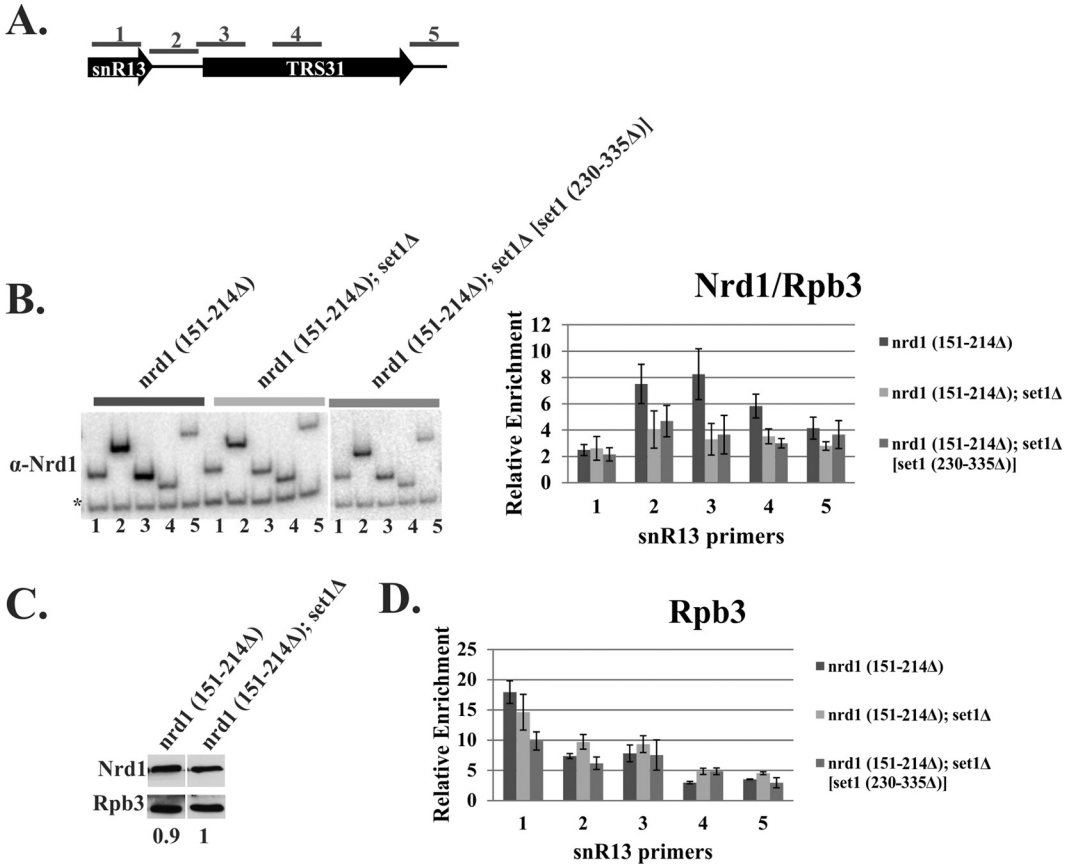


FIG. 4. Cells lacking Set1 have reduced Nrd1 recruitment to snoRNAs. (A) Schematic representation of the chromatin immunoprecipitation (ChIP) PCR probes spanning the *SNR13* region. See Table 2 for primer names and sequences. (B) ChIP analysis of *SNR13* using anti-Nrd1 antibody was carried out with *nrd1*(*151–214*Δ) (YSB2086), *nrd1*(*151–214*Δ) *set1*Δ (YSB2152), and *nrd1*(*151–214*Δ) *set1*(*230–335*Δ) (YSB2503) cells. (Left) Representative ChIP gel. The asterisk denotes a PCR product from a nontranscribed region used as a background control for normalization. (Right) Quantitation of data from three independent experiments normalized to anti-Rpb3 ChIPs (see panel D) using the same chromatin samples. Error bars indicate standard errors. (C) Immunoblot analysis of Nrd1 (antihemagglutinin) and Rpb3 levels in *nrd1*(*151-214*Δ) (YSB2086) and *nrd1*(*151-214*Δ) *set1*Δ (YSB2152) cells. Twenty micrograms of whole-cell extract from each strain was resolved on 12% SDS-PAGE gels. The quantitation of Nrd1 protein levels is shown below the blots. (D) Quantitation of three independent anti-Rpb3 ChIP experiments with *nrd1*(*151-214*Δ) (YSB2086), *nrd1*(*151-214*Δ) *set1*Δ (YSB2152), and *nrd1*(*151-214*Δ) *set1*(*230-335*Δ) (YSB2503) cells.

erally contributes to termination at snoRNAs and CUTs. Pho23 also appears to be important for snoRNA termination but perhaps less so at CUTs.

Since the read-through transcription of *SNR13* takes Pol II through the promoter region of *TRS31*, it could be argued that the termination defect in *set1*Δ or *pho23*Δ cells is due to changes at the *TRS31* promoter. However, *SNR3*, *SNR71*, *SNR9*, and *SNR128* are transcribed convergently with their downstream genes yet are still sensitive to the deletion of *PHO23* or *SET1* (Fig. 6). This finding rules out the possibility that the termination effects are due to Set1-mediated chromatin changes at a downstream promoter.

Our results are most consistent with a role for Set1 in snoRNA termination rather than 3′-end processing. ChIP experiments with *nrd1 set1* double mutant cells showed increased Rpb3 levels downstream of the normal termination site relative to the promoter, which is indicative of a termination defect (Fig. 4D). Additionally, the polyadenylated snR13-TRS31 read-through transcript is not subject to Nrd1/exosome-dependent processing but shows increased accumulation in *set1*Δ cells (Fig. 2A). To definitively demonstrate a role for Set1 in promoting Nrd1-dependent termination, nascent elongating transcript sequencing (NET-Seq) was carried out on *SET1* versus *set1*Δ cells. This technique identifies the precise 3′ ends of transcripts associated with elongating Pol II complexes, before 3′-end processing or degradation complicates analyses (14). The deletion of *SET1* had little effect on the abundance of sequence reads within the body of genes (mRNA or snoRNA) or downstream of mRNA termination sites (data not shown). In contrast, a notable increase in transcription downstream of snoRNA termination sites was observed for *set1*Δ cells (Fig. 7A). Similarly, there was also increased transcription downstream of the NEL025C CUT and the FMP40 CUT (Fig. 7B). These NET-Seq results confirm that the ChIP (Fig. 4D) and RT-PCR (Fig. 6) results reflect a role for Set1 in promoting Nrd1-dependent termination.

Kinetics of transcription affect snoRNA termination. Both *set1*Δ and *pho23*Δ cells are sensitive to 6-azauracil (6-AU), a drug that depletes the cellular GTP and UTP pools (24, 66). This phenotype is often seen with mutations in positive transcription elongation factors. We therefore wondered whether the termination defect caused by Set1 and Pho23 could be

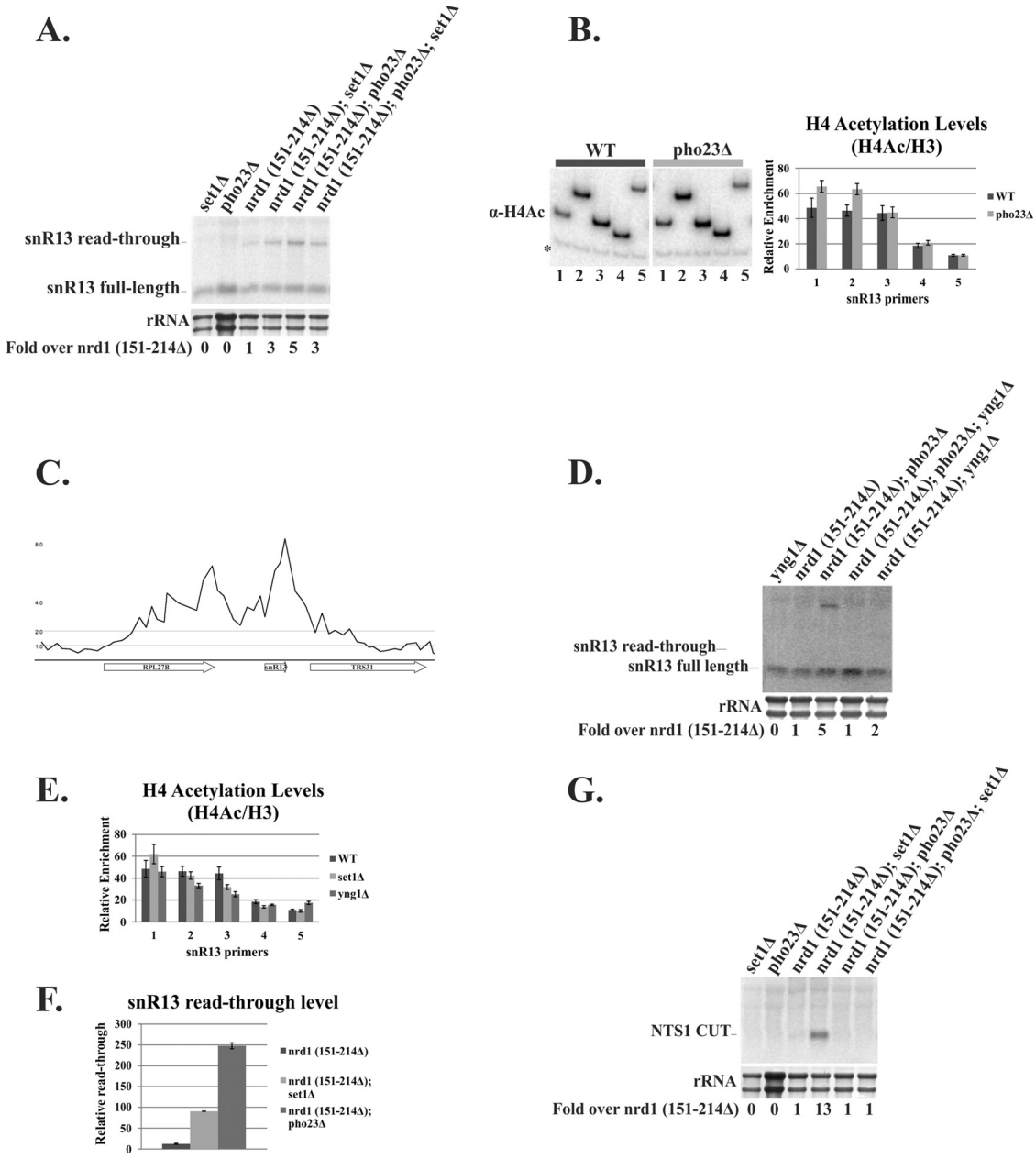


FIG. 5. Increased histone acetylation levels in *pho23*Δ cells enhance the termination defects of *nrd1* mutants. (A) Northern blot analysis of total RNA (5 μg) extracted from *set1*Δ (YSB2253), *pho23*Δ (YF688), *nrd1*(*151–214*Δ) (YSB2086), *nrd1*(*151–214*Δ) *set1*Δ (YSB2152), *nrd1*(*151–214*Δ) *pho23*Δ (YSB2412), and *nrd1*(*151–214*Δ) *pho23*Δ *set1*Δ (YSB2420) strains was carried out and quantitated as described in the legend of Fig. 2. (B) ChIP analysis of *SNR13* using anti-tetra-acetyl H4 antibody was carried out with WT (BY4741) and *pho23*Δ (YF688) cells. (Left) Representative ChIP gel, with the asterisk denoting a PCR product from a nontranscribed control region. (Right) Quantitation of three independent experiments normalized to anti-H3 ChIP data. Error bars indicate standard errors. (C) ChIP-chip trace for Rpd3-Myc for the snR13 region. Data were reported previously by Bumgarner et al. (7) and are accessible through ArrayExpress accession number E-MEXP-2269. (D) Northern blot analysis of total RNA extracted from *yng1*Δ (YF1495), *nrd1*(*151–214*Δ) (YSB2086), *nrd1*(*151–214*Δ) *pho23*Δ (YSB2412), *nrd1*(*151–214*Δ) *pho23 yng1*Δ (YSB2492), and *nrd1*(*151–214*Δ) *yng1*Δ (YSB2489) strains and probed for snR13. The positions of mature full-length snR13 and snR13-TRS31 read-through transcripts are indicated on the left. The quantitation of the snR13 read-through transcript level is expressed as described in the legend of Fig. 2. (E) Quantitation of three independent anti-tetra-acetyl H4 ChIP experiments of *snR13* in WT (BY4741), *set1*Δ (YSB2253), and *yng1*Δ (YF1495) cells. Error bars represent standard errors. (F) RT-PCR of snR13 read-through (26 cycles) and total (full-length plus read-through) transcripts (20 cycles) performed by using three independent cultures of *nrd1*(*151–214*Δ) (YSB2086), *nrd1*(*151–214*Δ) *set1*Δ (YSB2152), and *nrd1*(*151–214*Δ) *pho23*Δ (YSB2412) strains. The quantitation was done by the normalization of the read-through signal to the total signal. This result was also verified by qPCR (see Fig. S1C in the supplemental material). (G) Northern blot analysis of RNA as in panel A except with the blot probed for the NTS1 CUT (position indicated on the left). The quantitation of the NTS1 CUT level as "fold over *nrd1*(*151–214*Δ)" is shown below the gels.

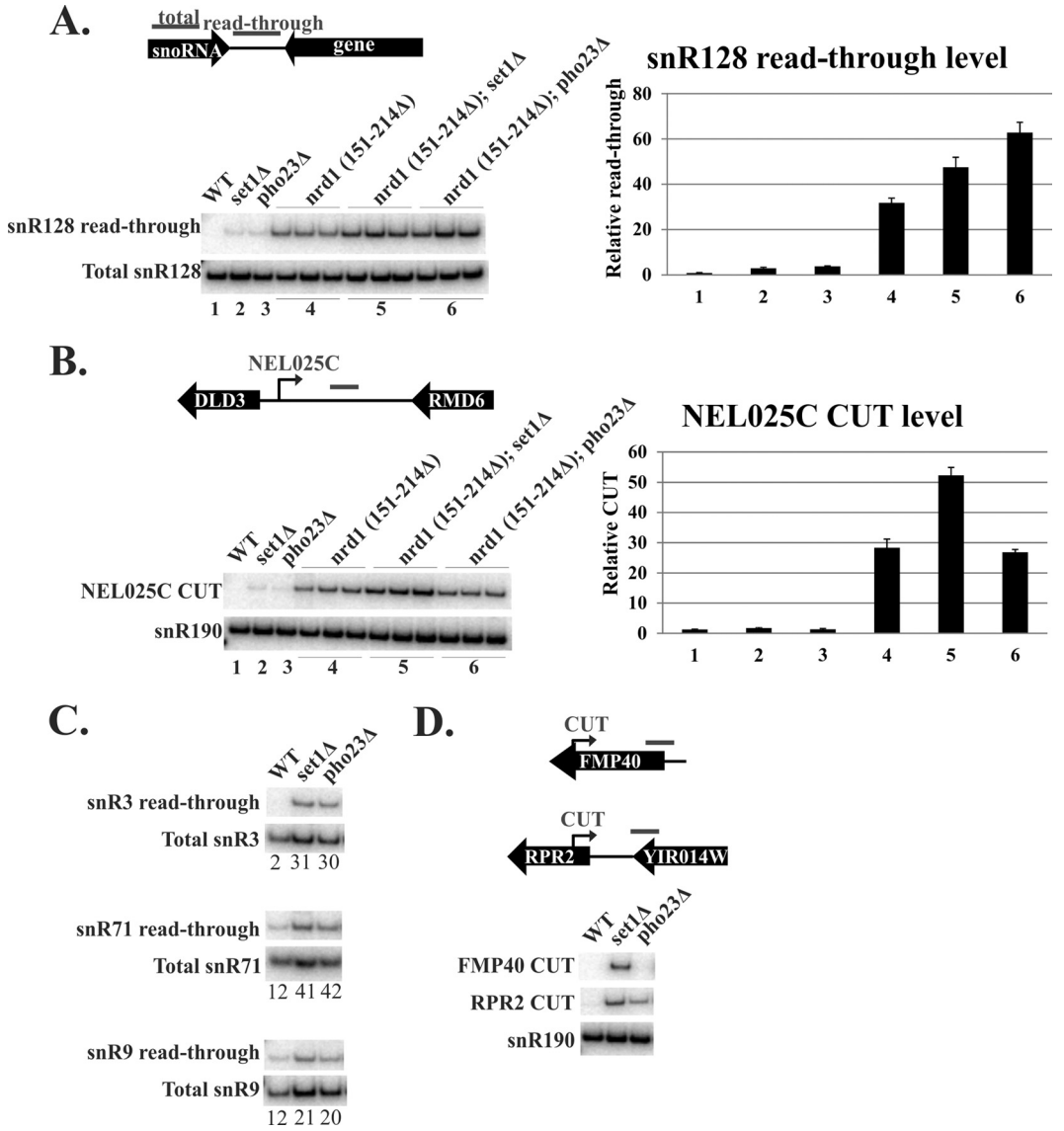


FIG. 6. Deletion of *SET1* or *PHO23* affects termination of multiple snoRNAs and CUTs. (A) RT-PCRs for snR128 read-through transcripts (26 cycles) and total (full-length plus read-through) transcripts (20 cycles) were performed by using WT (BY4741), *set1*Δ (YSB2253) *pho23*Δ (YF688), *nrd1*(*151–214*Δ) (YSB2086), *nrd1*(*151–214*Δ) *set1*Δ (YSB2152), and *nrd1*(*151–214*Δ) *pho23*Δ (YSB2412) strains. The schematic above the gel represents the position of read-through and total primer pairs used for the PCRs of snoRNAs. The graph on the right shows the quantitation of the snR128 read-through signal relative to the total snR128 transcript signal. The *x* axis indicates the strains used, designated below the gels. Error bars indicate standard errors from three biological replicates. (B) RT-PCRs for the NEL025C CUT (30 cycles) and snR190 transcripts (20 cycles) performed as described above for panel A. The schematic above the gel shows the position of the NEL025C initiation site (arrow) and the primer pair used for the PCRs. The snR190 signal shows total transcript levels that do not change with defects in the Nrd1 termination pathway and was therefore used for normalization. The graph on the right shows the quantitation of the NEL025C CUT signal relative to snR190. *x* axis numbers refer to the numbered lanes at the left. (C) RT-PCRs for snR3, snR71, and snR9 read-through transcripts (30 cycles) and total (full-length plus read-through) transcripts (20 cycles) were performed with WT (BY4741), *set1*Δ (YSB2253), and *pho23*Δ (YF688) strains. The numbers below each panel represent the quantitation of read-through signal relative to total transcript signal levels. (D) RT-PCRs for the *FMP40* CUT (30 cycles), the *RPR2* CUT (30 cycles), and snR190 total transcripts (20 cycles) were performed as in panel C. The schematic above the gels shows the positions of the CUT initiation site and the primer pairs used for the PCRs.

related to an effect on the Pol II elongation rate. The *rpb2-10* allele has a point mutation in a region important for nucleotide triphosphate binding, resulting in a polymerase that is slow and prone to arrest (36, 43). The combination of *rpb2-10* with either the *nrd1*(*151–214*Δ) *set1*Δ or the *nrd1*(*151–214*Δ) *pho23*Δ mutation resulted in increased snR13 read-through (Fig. 8A and see Fig. S1D in the supplemental material) and a decreased growth rate (Fig. 8B). Therefore, the slower Pol II elongation can decrease the efficiency of Nrd1-dependent termination and suggests a possible model for how Set1 and Pho23 influence this process (see below).

DISCUSSION

The early stages of RNA Pol II transcription elongation are marked by several events that are linked to CTD Ser5 phos-

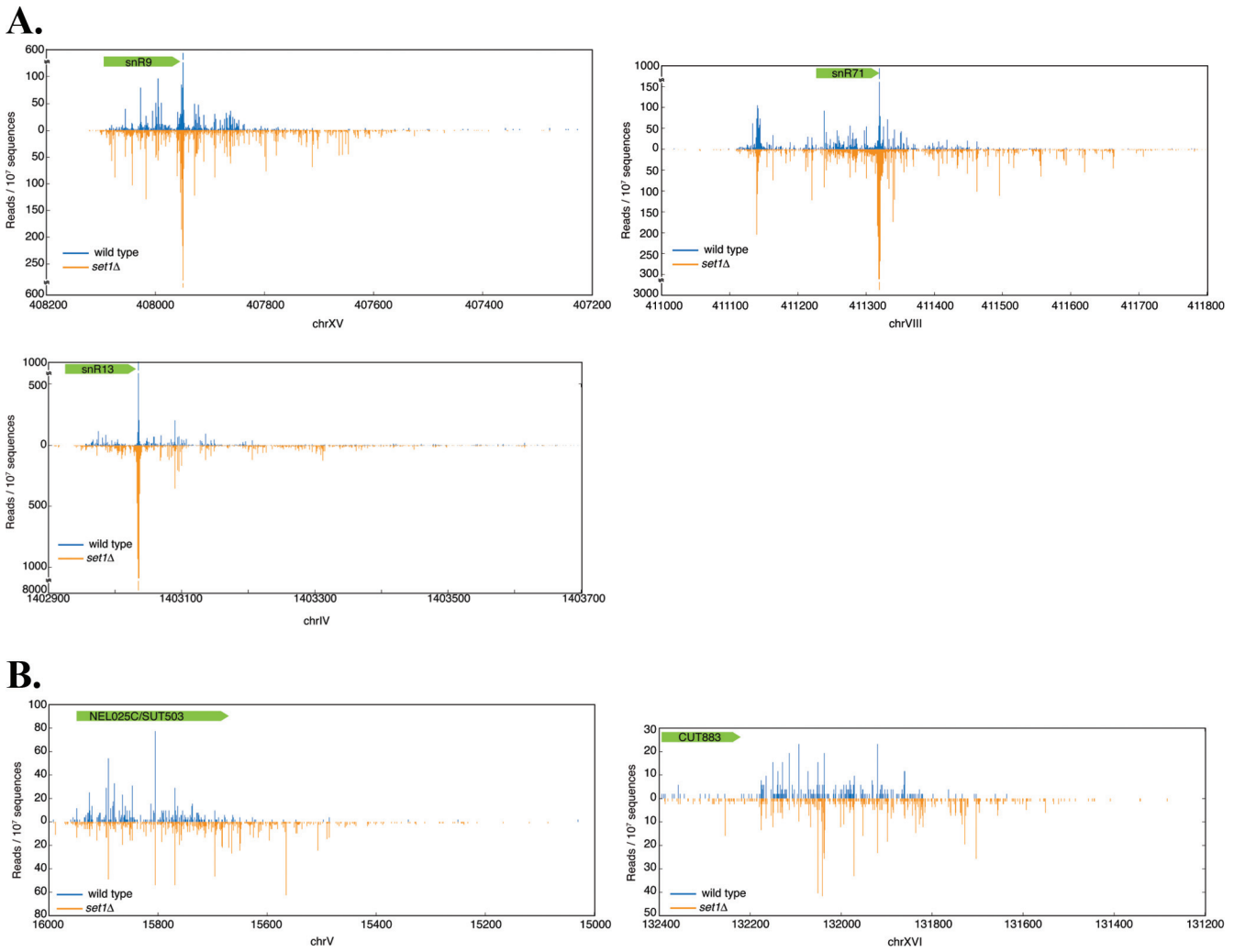


FIG. 7. NET-Seq analysis of *set1*Δ cells. (A) Sequenced 3′ ends of nascent transcripts from WT (BY4741) and *set1*Δ cells were mapped to the chromosomal (chr) locations of snoRNAs. The *x* axis shows the positions of nucleotides along the corresponding chromosome. The *y* axis shows the number of sequence reads for each nucleotide position in WT (blue, above zero) or *set1*Δ (orange, below zero) cells. The positions of snR9 (top left), snR71 (top right), and snR13 (bottom) are shown above each graph. (B) NET-Seq results for the NEL025C CUT (left) and *FMP40*-proximal CUT883 (right).

phorylation (8). These events include mRNA capping, higher levels of histone H3K4 methylation, and an early termination pathway in yeast that is mediated by Nrd1, Nab3, and Sen1. The Nrd1 complex mediates both transcription termination and the subsequent recruitment of the nuclear exosome for snoRNA 3′-end trimming (51, 59). This complex can be recruited to genes via multiple mechanisms, including the recognition of specific RNA sequences by Nrd1 and Nab3, or by the interaction of the Nrd1 CID with CTD S5P. It is likely that individual genes will vary in being more or less dependent on each of these recruitment pathways.

Here we demonstrate that H3K4 trimethylation, a mark associated with active transcription, also contributes to efficient termination by the Nrd1/Sen1 pathway. The deletion of *SET1* either by itself or in an *nrd1* mutant background enhances the termination read-through of several snoRNAs and CUTs tested (Fig. 2A and D, 5F, 6, and 7). Although these effects are much less than those seen for mutants of the actual termination factors themselves, our results indicate that chromatin modifications near promoters can influence the choice of whether to terminate soon after initiation or to continue elongating.

Interestingly, mutations in the Paf1 complex have also been reported to cause snoRNA termination defects by reducing the recruitment of the Nrd1 complex (48). Since the Paf1 complex is required for proper H3K4 methylation by Set1, it is logical to ask whether the Paf1 complex effect might be mediated via Set1. Sheldon et al. (48) concluded that this was unlikely because snR13 read-through transcripts were not seen in a *SET1* deletion. While this clearly suggests that the Paf1 complex has additional functions related to snoRNA termination, our observations of read-through transcripts in *set1*Δ cells make it worth revisiting the idea that some of the Paf1 complex occurs via a disruption of H3K4 methylation. We note that while this paper was under review, a follow-up study by the Arndt laboratory

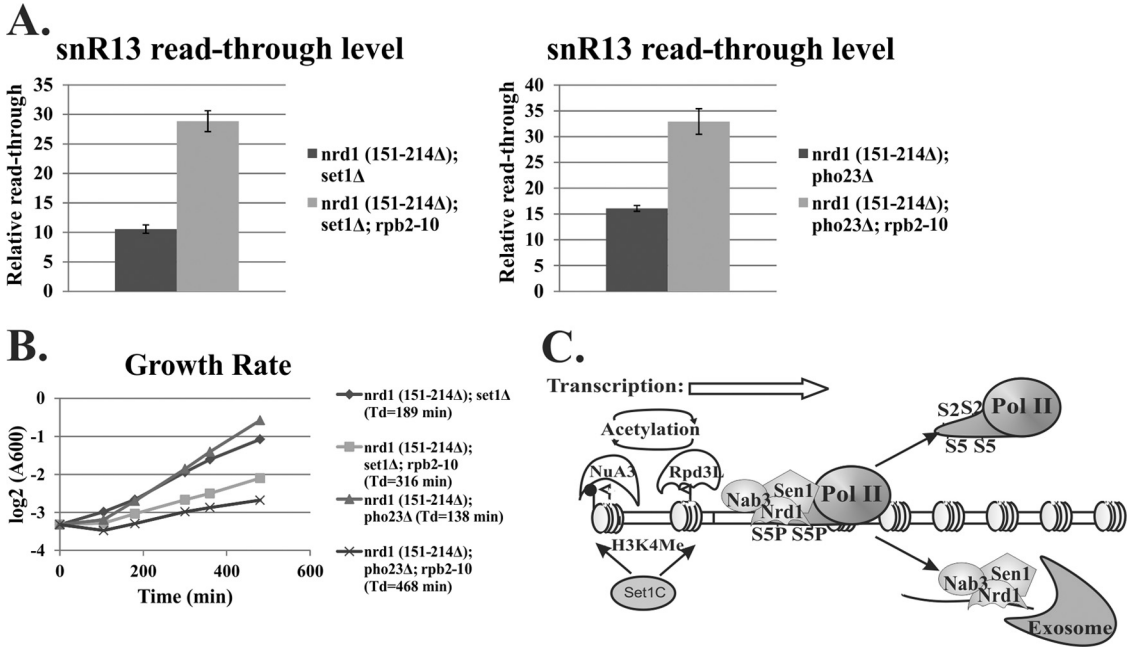


FIG. 8. Pol II kinetics can affect Nrd1-dependent termination. (A) RT-PCRs for snR13 read-through (26 cycles) and total (full-length plus read-through) transcripts (20 cycles) were performed by using three independent cultures of *nrd1*(*151–214*Δ) *set1*Δ (YSB2582) and *nrd1*(*151–214*Δ) *set1*Δ *rpb2-10* (YSB2583) (left) or *nrd1*(*151–214*Δ) *pho23*Δ (YSB2574) and *nrd1*(*151–214*Δ) *pho23*Δ *rpb2-10* (YSB2595) (right) strains. The graphs show the quantitation as read-through signal relative to the total signal. These results were also confirmed by qPCR (see Fig. S1D in the supplemental material). (B) Growth rates of *nrd1*(*151–214*Δ) *set1*Δ (YSB2582), *nrd1*(*151–214*Δ) *set1*Δ *rpb2-10* (YSB2583), *nrd1*(*151–214*Δ) *pho23*Δ (YSB2574), and *nrd1*(*151–214*Δ) *pho23*Δ *rpb2-10* (YSB2595) strains were assayed in liquid synthetic complete medium at 30°C starting from an A_{600} of 0.1. The graph key shows the calculated doubling time (Td) of each strain in parentheses. (C) Proposed model for how H3K4me3 in the promoter-proximal region affects histone acetylation and the early termination pathway. The NuA3 acetyltransferase complex may recognize H3K4me3 via the Yng1 PHD finger. Similarly, the Pho23 PHD finger may bring the Rpd3L deacetylase complex to H3K4me3-modified nucleosomes at active promoters. The actions of these two complexes maintain an optimum level of histone acetylation (black circles), which promotes proper Nrd1-dependent termination by affecting the kinetics of early Pol II elongation.

showed that the termination defect observed for Paf1 complex mutants is likely mediated via its effect on H2B ubiquitylation (57), a prerequisite for H3K4 trimethylation.

The contribution to Nrd1-dependent termination by Set1 is clearly related to its histone methyltransferase activity. Histone H3 mutated at lysine 4 (Fig. 3F) or a catalytic-site mutant of Set1 (Fig. 3A to D) produced effects similar to those seen in *set1*Δ cells. It appears that it is specifically H3K4 trimethylation that promotes Nrd1-dependent termination. The monoubiquitylation of H2BK123 by the Rad6/Bre1 complex, which is required for H3K4 di- and trimethylation by Set1 (29, 53), also promotes efficient Nrd1-dependent transcription termination (Fig. 3E) (57). Similarly, the *set1*(*230–335*Δ) allele, which abolishes H3K4 trimethylation but not H3K4 dimethylation (see Fig. S2 in the supplemental material) (18, 26), also exhibits a reduction of Nrd1 recruitment with subsequent termination defects (Fig. 3C and D and 4B). Given that snoRNAs and CUTs are terminated relatively close to the promoter, it makes sense that promoter-proximal H3K4 trimethylation would be linked to the Nrd1-Nab3-Sen1 termination pathway.

Set1 may promote *SNR13* termination by affecting histone acetylation levels. Because the deletion of *PHO23* also leads to read-through, we suspect that this effect occurs via the Rpd3L HDAC. Although sequence-specific DNA binding proteins such as Ume6 can recruit Rpd3L to repress specific promoters (12, 22, 27, 47), we speculate that the PHD fingers of the Rpd3L subunits Pho23 and Cti6 can bind H3K4me3 to moderate acetylation levels at active promoters. This model is supported by several findings. First, cells lacking Pho23 show a small but significant increase in acetylation at the *SNR13* (Fig. 5B) and YEF3 (18, 26) promoters. Additionally, Rpd3 recruitment was observed in *SNR13* and *SNR128* regions (Fig. 5C and see Fig. S3A in the supplemental material) (data from reference 7) where *pho23*Δ results in termination defects (Fig. 5A and 6A). Another genome-wide ChIP analysis of Rpd3 showed that, in addition to being recruited to a small group of repressed promoters, the deacetylase was unexpectedly found to cross-link to active promoters proportional to their transcription rate (27). At the time, those authors speculated that Rpd3 might be recruited to active promoters to dampen high levels of acetylation. A similar story emerged from genome-wide mapping of HATs and HDACs in mammalian cells. HDACs are recruited to active genes, and levels correlated positively with H3K4 methylation (63). Therefore, both HATs and HDACs may functionally associate with active promoters. Supporting this view, we show that the blocking of NuA3 HAT recruitment by the deletion of *YNG1* reverses the enhancement of the termination defect by *pho23*Δ (Fig. 5D). Although it may appear paradoxical for H3K4me3 to recruit the antagonistic activities of both NuA3 (via Yng1) and Rpd3L (via Pho23 and Cti6) to the promoter, this mechanism may maintain balanced levels of histone acetylation or perhaps allow

cycles of acetylation and deacetylation that are important for proper transcription.

In yeast, the choice between early Nrd1-dependent termination or continued elongation to downstream polyadenylation sites must be made for both snoRNAs and mRNA genes (8). Set1 may influence this decision point by affecting the kinetics of early transcription (Fig. 8). This idea is supported by the sensitivity of *set1*Δ or *pho23*Δ cells to 6-AU as well as the genetic interaction with a *RPB2* allele that slows elongation. The loss of H3K4 trimethylation may make it slightly harder for Pol II to travel through the promoter-proximal chromatin environment, perhaps due to downstream effects on nucleosome acetylation or remodeling. A slower transit time through this window might affect the modifications of Pol II or the recruitment of necessary elongation factors, resulting in termination defects for snoRNAs and CUTs. The recent observation that another slow Pol II allele, *rpb1*(*N488D*), shows reduced capping efficiency (21) supports this concept. Although recent reports failed to detect widespread mRNA changes in the absence of Set1 (18, 46, 62), it is possible that a subset of genes could be affected by this mechanism.

A choice between early or late termination pathways might also underlie the regulation of genes in higher eukaryotes, where higher levels of Pol II accumulate near the 5′ ends of genes relative to further downstream (34). While some of these promoter-proximal polymerase molecules may be paused, others may be destined for early termination (8). It was recently found that bidirectional transcription is an inherent feature of many actively transcribed genes (reviewed in reference 9). In yeast, the reverse-direction promoter-associated transcripts are terminated by the Nrd1-Nab3-Sen1 complex (40). It will be interesting to see whether H3K4 methylation also plays a role in mediating early pausing and termination in metazoans.

ACKNOWLEDGMENTS

We thank G. Fink and S. Bumgarner for sharing their Rpd3-Myc ChIP-chip data, J. Corden (JHMI) for anti-Nrd1 antibody and Nrd1 plasmids, S. Briggs (Purdue) for Set1 partial deletion constructs, and R. Buratowski for help with the tables in the supplemental material. We also thank T. S. Kim, D. Hazelbaker, and M. C. Keogh (AECOM) for critical reading of the manuscript.

L.S.C. was supported by the Damon Runyon Cancer Research Foundation. This work was supported by NIH grants GM46498 and GM56663 to S.B.

REFERENCES

1. **Ahn, S. H., M. Kim, and S. Buratowski.** 2004. Phosphorylation of serine 2 within the RNA polymerase II C-terminal domain couples transcription and 3′ end processing. Mol. Cell **13:**67–76.
2. **Alen, C., et al.** 2002. A role for chromatin remodeling in transcriptional termination by RNA polymerase II. Mol. Cell **10:**1441–1452.
3. **Arigo, J. T., D. E. Eyler, K. L. Carroll, and J. L. Corden.** 2006. Termination of cryptic unstable transcripts is directed by yeast RNA-binding proteins Nrd1 and Nab3. Mol. Cell **23:**841–851.
4. **Bartkowiak, B., et al.** 2010. CDK12 is a transcription elongation-associated CTD kinase, the metazoan ortholog of yeast Ctk1. Genes Dev. **24:**2303–2316.
5. **Biswas, D., et al.** 2006. Opposing roles for Set2 and yFACT in regulating TBP binding at promoters. EMBO J. **25:**4479–4489.
6. **Briggs, S. D., et al.** 2001. Histone H3 lysine 4 methylation is mediated by Set1 and required for cell growth and rDNA silencing in Saccharomyces cerevisiae. Genes Dev. **15:**3286–3295.
7. **Bumgarner, S. L., R. D. Dowell, P. Grisafi, D. K. Gifford, and G. R. Fink.** 2009. Toggle involving cis-interfering noncoding RNAs controls variegated gene expression in yeast. Proc. Natl. Acad. Sci. U. S. A. **106:**18321–18326.
8. **Buratowski, S.** 2009. Progression through the RNA polymerase II CTD cycle. Mol. Cell **36:**541–546.
9. **Carninci, P.** 2009. Molecular biology: the long and short of RNAs. Nature **457:**974–975.
10. **Carroll, K. L., D. A. Pradhan, J. A. Granek, N. D. Clarke, and J. L. Corden.** 2004. Identification of cis elements directing termination of yeast nonpolyadenylated snoRNA transcripts. Mol. Cell. Biol. **24:**6241–6252.
11. **Carrozza, M. J., et al.** 2005. Histone H3 methylation by Set2 directs deacetylation of coding regions by Rpd3S to suppress spurious intragenic transcription. Cell **123:**581–592.
12. **Chang, C. S., and L. Pillus.** 2009. Collaboration between the essential Esa1 acetyltransferase and the Rpd3 deacetylase is mediated by H4K12 histone acetylation in Saccharomyces cerevisiae. Genetics **183:**149–160.
13. **Cho, E. J., M. S. Kobor, M. Kim, J. Greenblatt, and S. Buratowski.** 2001. Opposing effects of Ctk1 kinase and Fcp1 phosphatase at Ser 2 of the RNA polymerase II C-terminal domain. Genes Dev. **15:**3319–3329.
14. **Churchman, L. S., and J. S. Weissman.** 2011. Nascent transcript sequencing visualizes transcription at nucleotide resolution. Nature **469:**368–373.
15. **Collins, S. R., et al.** 2007. Functional dissection of protein complexes involved in yeast chromosome biology using a genetic interaction map. Nature **446:**806–810.
16. **Conrad, N. K., et al.** 2000. A yeast heterogeneous nuclear ribonucleoprotein complex associated with RNA polymerase II. Genetics **154:**557–571.
17. **Dahmus, M. E.** 1996. Reversible phosphorylation of the C-terminal domain of RNA polymerase II. J. Biol. Chem. **271:**19009–19012.
18. **Fingerman, I. M., C. L. Wu, B. D. Wilson, and S. D. Briggs.** 2005. Global loss of Set1-mediated H3 Lys4 trimethylation is associated with silencing defects in Saccharomyces cerevisiae. J. Biol. Chem. **280:**28761–28765.
19. **Howe, L., et al.** 2002. Yng1p modulates the activity of Sas3p as a component of the yeast NuA3 histone acetyltransferase complex. Mol. Cell. Biol. **22:**5047–5053.
20. Reference deleted.
21. **Jimeno-Gonzalez, S., L. L. Haaning, F. Malagon, and T. H. Jensen.** The yeast 5′-3′ exonuclease Rat1p functions during transcription elongation by RNA polymerase II. Mol. Cell **37:**580–587.
22. **Kadosh, D., and K. Struhl.** 1998. Targeted recruitment of the Sin3-Rpd3 histone deacetylase complex generates a highly localized domain of repressed chromatin in vivo. Mol. Cell. Biol. **18:**5121–5127.
23. **Keogh, M. C., and S. Buratowski.** 2004. Using chromatin immunoprecipitation to map cotranscriptional mRNA processing in Saccharomyces cerevisiae. Methods Mol. Biol. **257:**1–16.
24. **Keogh, M. C., et al.** 2005. Cotranscriptional set2 methylation of histone H3 lysine 36 recruits a repressive Rpd3 complex. Cell **123:**593–605.
25. **Kim, M., et al.** 2006. Distinct pathways for snoRNA and mRNA termination. Mol. Cell **24:**723–734.
26. **Kim, T., and S. Buratowski.** 2009. Dimethylation of H3K4 by Set1 recruits the Set3 histone deacetylase complex to 5′ transcribed regions. Cell **137:**259–272.
27. **Kurdistani, S. K., D. Robyr, S. Tavazoie, and M. Grunstein.** 2002. Genome-wide binding map of the histone deacetylase Rpd3 in yeast. Nat. Genet. **31:**248–254.
28. **Larochelle, S., et al.** 2006. Dichotomous but stringent substrate selection by the dual-function Cdk7 complex revealed by chemical genetics. Nat. Struct. Mol. Biol. **13:**55–62.
29. **Lee, J. S., et al.** 2007. Histone crosstalk between H2B monoubiquitination and H3 methylation mediated by COMPASS. Cell **131:**1084–1096.
30. **Li, B., et al.** 2007. Infrequently transcribed long genes depend on the Set2/Rpd3S pathway for accurate transcription. Genes Dev. **21:**1422–1430.
31. **Liu, Y., et al.** 2004. Two cyclin-dependent kinases promote RNA polymerase II transcription and formation of the scaffold complex. Mol. Cell. Biol. **24:**1721–1735.
32. **Loewith, R., M. Meijer, S. P. Lees-Miller, K. Riabowol, and D. Young.** 2000. Three yeast proteins related to the human candidate tumor suppressor p33(ING1) are associated with histone acetyltransferase activities. Mol. Cell. Biol. **20:**3807–3816.
33. **Loewith, R., et al.** 2001. Pho23 is associated with the Rpd3 histone deacetylase and is required for its normal function in regulation of gene expression and silencing in Saccharomyces cerevisiae. J. Biol. Chem. **276:**24068–24074.
34. **Margaritis, T., and F. C. Holstege.** 2008. Poised RNA polymerase II gives pause for thought. Cell **133:**581–584.
35. **Martin, D. G., et al.** 2006. The Yng1p plant homeodomain finger is a methyl-histone binding module that recognizes lysine 4-methylated histone H3. Mol. Cell. Biol. **26:**7871–7879.
36. **Mason, P. B., and K. Struhl.** 2005. Distinction and relationship between elongation rate and processivity of RNA polymerase II in vivo. Mol. Cell **17:**831–840.
37. **Moazed, D.** 2001. Common themes in mechanisms of gene silencing. Mol. Cell **8:**489–498.
38. **Moazed, D.** 2001. Enzymatic activities of Sir2 and chromatin silencing. Curr. Opin. Cell Biol. **13:**232–238.
39. **Morillon, A., et al.** 2003. Isw1 chromatin remodeling ATPase coordinates transcription elongation and termination by RNA polymerase II. Cell **115:**425–435.

40. **Neil, H., et al.** 2009. Widespread bidirectional promoters are the major source of cryptic transcripts in yeast. Nature **457:**1038–1042.
41. **Ng, H. H., F. Robert, R. A. Young, and K. Struhl.** 2003. Targeted recruitment of Set1 histone methylase by elongating Pol II provides a localized mark and memory of recent transcriptional activity. Mol. Cell **11:**709–719.
42. **Pokholok, D. K., et al.** 2005. Genome-wide map of nucleosome acetylation and methylation in yeast. Cell **122:**517–527.
43. **Powell, W., and D. Reines.** 1996. Mutations in the second largest subunit of RNA polymerase II cause 6-azauracil sensitivity in yeast and increased transcriptional arrest in vitro. J. Biol. Chem. **271:**6866–6873.
44. **Qiu, H., C. Hu, and A. G. Hinnebusch.** 2009. Phosphorylation of the Pol II CTD by KIN28 enhances BUR1/BUR2 recruitment and Ser2 CTD phosphorylation near promoters. Mol. Cell **33:**752–762.
45. **Scafe, C., et al.** 1990. Conditional mutations occur predominantly in highly conserved residues of RNA polymerase II subunits. Mol. Cell. Biol. **10:**1270–1275.
46. **Schlichter, A., and B. R. Cairns.** 2005. Histone trimethylation by Set1 is coordinated by the RRM, autoinhibitory, and catalytic domains. EMBO J. **24:**1222–1231.
47. **Sharma, V. M., R. S. Tomar, A. E. Dempsey, and J. C. Reese.** 2007. Histone deacetylases RPD3 and HOS2 regulate the transcriptional activation of DNA damage-inducible genes. Mol. Cell. Biol. **27:**3199–3210.
48. **Sheldon, K. E., D. M. Mauger, and K. M. Arndt.** 2005. A requirement for the Saccharomyces cerevisiae Paf1 complex in snoRNA 3′ end formation. Mol. Cell **20:**225–236.
49. **Shi, X., et al.** 2007. Proteome-wide analysis in Saccharomyces cerevisiae identifies several PHD fingers as novel direct and selective binding modules of histone H3 methylated at either lysine 4 or lysine 36. J. Biol. Chem. **282:**2450–2455.
50. **Steinmetz, E. J., and D. A. Brow.** 1998. Control of pre-mRNA accumulation by the essential yeast protein Nrd1 requires high-affinity transcript binding and a domain implicated in RNA polymerase II association. Proc. Natl. Acad. Sci. U. S. A. **95:**6699–6704.
51. **Steinmetz, E. J., N. K. Conrad, D. A. Brow, and J. L. Corden.** 2001. RNA-binding protein Nrd1 directs poly(A)-independent 3′-end formation of RNA polymerase II transcripts. Nature **413:**327–331.
52. **Steinmetz, E. J., et al.** 2006. Genome-wide distribution of yeast RNA polymerase II and its control by Sen1 helicase. Mol. Cell **24:**735–746.
53. **Sun, Z. W., and C. D. Allis.** 2002. Ubiquitination of histone H2B regulates H3 methylation and gene silencing in yeast. Nature **418:**104–108.
54. **Sun, Z. W., and M. Hampsey.** 1999. A general requirement for the Sin3-Rpd3 histone deacetylase complex in regulating silencing in Saccharomyces cerevisiae. Genetics **152:**921–932.
55. **Taverna, S. D., et al.** 2006. Yng1 PHD finger binding to H3 trimethylated at K4 promotes NuA3 HAT activity at K14 of H3 and transcription at a subset of targeted ORFs. Mol. Cell **24:**785–796.
56. **Thiebaut, M., E. Kisseleva-Romanova, M. Rougemaille, J. Boulay, and D. Libri.** 2006. Transcription termination and nuclear degradation of cryptic unstable transcripts: a role for the nrd1-nab3 pathway in genome surveillance. Mol. Cell **23:**853–864.
57. **Tomson, B. N., C. P. Davis, M. H. Warner, and K. M. Arndt.** 2011. Identification of a role for histone H2B ubiquitylation in noncoding RNA 3′-end formation through mutational analysis of Rtf1 in Saccharomyces cerevisiae. Genetics **188:**273–289.
58. **Tresaugues, L., et al.** 2006. Structural characterization of Set1 RNA recognition motifs and their role in histone H3 lysine 4 methylation. J. Mol. Biol. **359:**1170–1181.
59. **Vasiljeva, L., and S. Buratowski.** 2006. Nrd1 interacts with the nuclear exosome for 3′ processing of RNA polymerase II transcripts. Mol. Cell **21:**239–248.
60. **Vasiljeva, L., M. Kim, H. Mutschler, S. Buratowski, and A. Meinhart.** 2008. The Nrd1-Nab3-Sen1 termination complex interacts with the Ser5-phosphorylated RNA polymerase II C-terminal domain. Nat. Struct. Mol. Biol. **15:**795–804.
61. **Vasiljeva, L., M. Kim, N. Terzi, L. M. Soares, and S. Buratowski.** 2008. Transcription termination and RNA degradation contribute to silencing of RNA polymerase II transcription within heterochromatin. Mol. Cell **29:**313–323.
62. **Venkatasubrahmanyam, S., W. W. Hwang, M. D. Meneghini, A. H. Tong, and H. D. Madhani.** 2007. Genome-wide, as opposed to local, antisilencing is mediated redundantly by the euchromatic factors Set1 and H2A.Z. Proc. Natl. Acad. Sci. U. S. A. **104:**16609–16614.
63. **Wang, Z., et al.** 2009. Genome-wide mapping of HATs and HDACs reveals distinct functions in active and inactive genes. Cell **138:**1019–1031.
64. **Winzeler, E. A., et al.** 1999. Functional characterization of the S. cerevisiae genome by gene deletion and parallel analysis. Science **285:**901–906.
65. **Yuryev, A., et al.** 1996. The C-terminal domain of the largest subunit of RNA polymerase II interacts with a novel set of serine/arginine-rich proteins. Proc. Natl. Acad. Sci. U. S. A. **93:**6975–6980.
66. **Zhang, L., S. Schroeder, N. Fong, and D. L. Bentley.** 2005. Altered nucleosome occupancy and histone H3K4 methylation in response to 'transcriptional stress'. EMBO J. **24:**2379–2390.